Journal of Medicinal Chemistry

pubs.acs.org/jmc

Article

Reduction of the Renal Radioactivity of ^{111}In-DOTA-Labeled Antibody Fragments with a Linkage Cleaved by the Renal Brush Border Membrane Enzymes

Published as part of the Journal of Medicinal Chemistry virtual special issue "Diagnostic and Therapeutic Radiopharmaceuticals".

Hiroyuki Suzuki,* Mari Araki, Kouki Tatsugi, Kento Ichinohe, Tomoya Uehara, and Yasushi Arano

Cite This: *J. Med. Chem.* 2023, 66, 8600−8613

Read Online

ACCESS | Metrics & More | Article Recommendations | Supporting Information

ABSTRACT: The interposition of a cleavable linkage by enzymes on the renal brush border membrane constitutes a promising approach for reducing the renal radioactivity levels of radiolabeled low-molecular-weight antibody fragments and constructs (LMW Abs). Herein, we applied the molecular design to 1,4,7,10-tetraazacyclododecane-1,4,7,10-tetraacetic acid (DOTA)-based reagents for radiotheranostic applications with trivalent radiometals. DOTA or a derivative thereof was conjugated to a Fab through an FGK linkage ([^{111}In]In-DO3A*i*Bu-Bn-FGK-Fab or [^{111}In]In-DOTA-Bn-FGK-Fab). When injected into mice, both generated radiometabolites, [^{111}In]In-DO3A*i*Bu-Bn-F and [^{111}In]In-DOTA-Bn-F, by the angiotensin-converting enzyme at similar rates. Both exhibited significantly lower renal radioactivity levels than a ^{111}In-labeled Fab prepared by the conventional procedure ([^{111}In]In-DOTA-Bn-SCN-Fab). The different elimination rates of each radiometabolite from the kidney significantly affected the renal radioactivity levels. [^{111}In]In-DO3A*i*Bu-Bn-FGK-Fab preferentially reduced the renal localization without impairing tumor accumulation. These findings would pave the way for developing a DOTA-based radiotheranostic platform for LMW Abs bearing cleavable linkers for renal brush border enzymes.

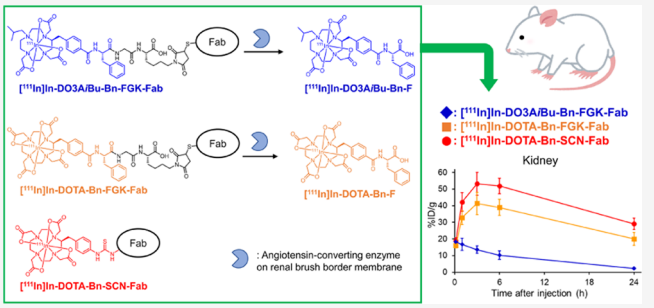

INTRODUCTION

Radiotheranostics is a combination of diagnostic and therapeutic radiopharmaceuticals on a single platform to facilitate the assessment of the safety, toxicity, and therapeutic efficacy of personalized medical approaches.[1] Zevalin therapy constitutes a typical example of radiotheranostics; the gamma camera imaging with [^{111}In]In-Zevalin is performed to confirm the expected biodistribution of [^{111}In]In-Zevalin before the administration of [^{90}Y]Y-Zevalin.[2] Various combinations of radiometals and biomolecules have been applied to radiotheranostics, such as ^{68}Ga/^{90}Y/^{177}Lu-labeled octreotide analogues and ^{68}Ga/^{177}Lu/^{225}Ac-labeled prostate-specific membrane antigen inhibitors.[3,4]

The effectiveness of the Zevalin regimen stimulated the development of various radiolabeled antibodies (Abs).[2,5] However, the radiolabeled Abs exhibit dose-limiting toxicity, predominantly myelotoxicity, due to slow elimination rates from the circulation. Meanwhile, low-molecular-weight antibody fragments and constructs (LMW Abs) such as Fab, Fv, and affibodies show more rapid blood clearance and evener distribution in the tumor than intact Abs. Such biological properties of LMW Abs are advantageous to achieve clear images shortly after injection, avoiding myelotoxicity and improving therapeutic effects.[6−9] However, high and persistent renal radioactivity levels are observed after injection of radiolabeled LMW Abs. Following glomerular filtration and subsequent reabsorption into renal cells, LMW Abs undergo lysosomal degradation to liberate the associated radiometabolites. The slow clearance of the final radiometabolites leads to undesirable radioactivity localization in the kidney.[10,11] Hence, this issue has been limiting further development of radiolabeled LMW Abs for over three decades.[12]

We had proposed a renal brush border strategy to tackle this issue.[13] In this strategy, a cleavable linkage introduced between a radiolabel and an LMW Ab-conjugation moiety is recognized by enzymes on the renal brush border membrane (BBM) to release a radiometabolite designed to be rapidly excreted into the urine. Based on this strategy, we developed a radioiodinated Fab with a

Received: February 14, 2023
Published: June 16, 2023

https://doi.org/10.1021/acs.jmedchem.3c00258
J. Med. Chem. 2023, 66, 8600−8613

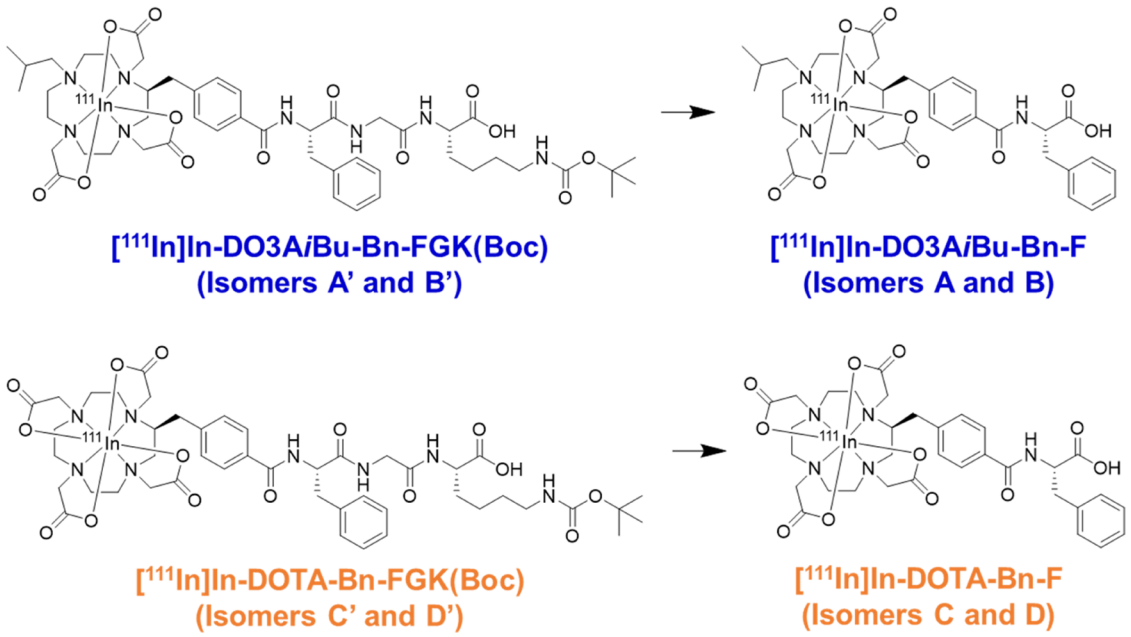

Figure 1. Molecular designs of ^{111}In-labeled LMW substrates used in this study. Both the LMW substrates and the authentic compounds generated a pair of isomers (Figure 3A). The metabolites were designed to be liberated by the action of ACE on the renal BBM.

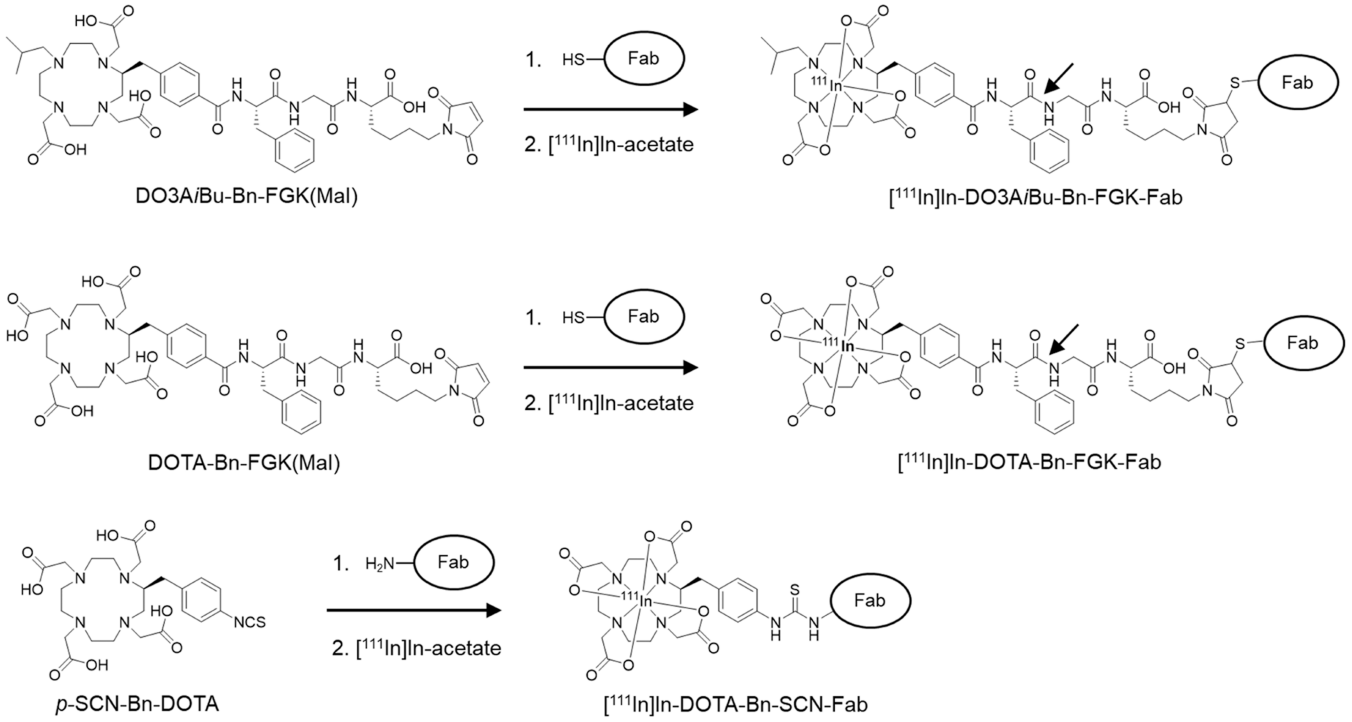

Figure 2. Synthetic procedures for ^{111}In-labeled Fabs used in this study. An FGK sequence was selected as a cleavable linkage to liberate the Phe adduct of the chelators as the radiometabolites. The arrows show the peptide bond expected to be cleaved by ACE. While [^{111}In]In-DOTA-Bn forms a net negative charged (−1) complex, [^{111}In]In-DO3A*i*Bu-Bn provides a neutral complex with a lipophilic isobutyl group. [^{111}In]In-DOTA-Bn-FGK-Fab was prepared by the conventional method and used as a reference.

cleavable GK linkage ([$^{125/131}$I]HML-IT-Fab).[14] The GK linkage was applied exceptionally to [^{188}Re]organorhenium-labeled Fab ([^{188}Re]Re-CpTR-GK-Fab).[15] However, the linkage failed to be recognized by the enzymes when applied to other radiometal chelates. This problem was cracked with tripeptide sequences cleaved by the action of neutral endopeptidase (NEP). These findings contributed to the development of [^{67}Ga]Ga/[^{64}Cu]Cu-NOTA-MVK-Fab, [^{99m}Tc]Tc-IPG-GFK-Fab, and [^{99m}Tc]Tc-MAG$_3$-GFK-Fab.[16−19]

1,4,7,10-Tetraazacyclododecane-1,4,7,10-tetraacetic acid (DOTA) is one of the current gold standard chelators for ^{111}In, ^{177}Lu, and $^{86/90}$Y, and has also been applied to other trivalent radiometals such as ^{68}Ga, ^{44}Sc, ^{225}Ac, and $^{212/213}$Bi.[20] Thus, DOTA offers the possibility of versatile radiotheranostic applications involving a combination of PET/SPECT imaging

https://doi.org/10.1021/acs.jmedchem.3c00258
J. Med. Chem. 2023, 66, 8600−8613

Scheme 1. Synthetic Procedure for *p*-COOH-Bn-DO3A*i*Bu(^{t}Bu)$_3$[a]

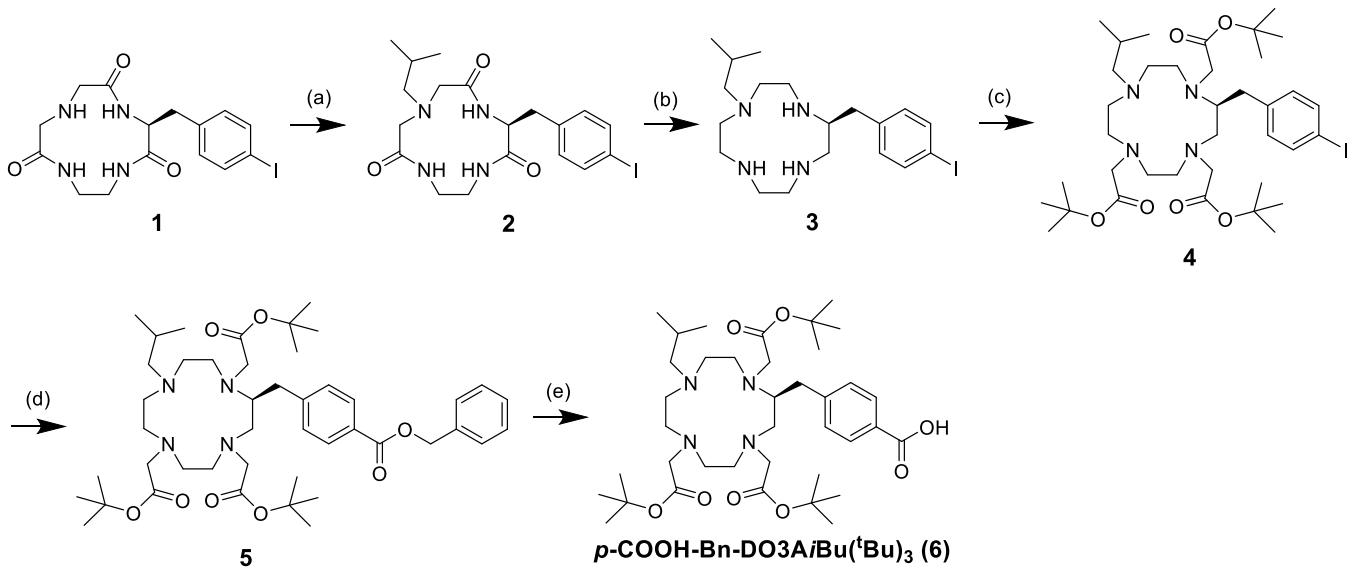

[a]Reagents and conditions: (a) isobutylaldehyde, sodium triacetoxyborohydride, THF, rt for 24 h, 42.4%; (b) (1) 1 M BH_3-THF, THF, 0 °C for 1 h, reflux for 24 h, 0 °C for 1 h, (2) conc. HCl, rt for 24 h, 74.7%; (c) *tert*-butyl bromoacetate, Na_2CO_3, acetonitrile, reflux for 24 h, 58.8%; (d) $Pd(OAc)_2$, 1,2-bis(diphenylphosphino)ethane, TEA, CO (1 atm), benzyl alcohol, DMF, 80 °C for 24 h, 25.5%; (e) 10% Pd/C, H_2 (1 atm), methanol, rt for 5 h, 48.8%.

Scheme 2. Synthetic Procedure for the Precursors for LMW Substrates and Bifunctional Chelating Agents with FGK Linkage[a]

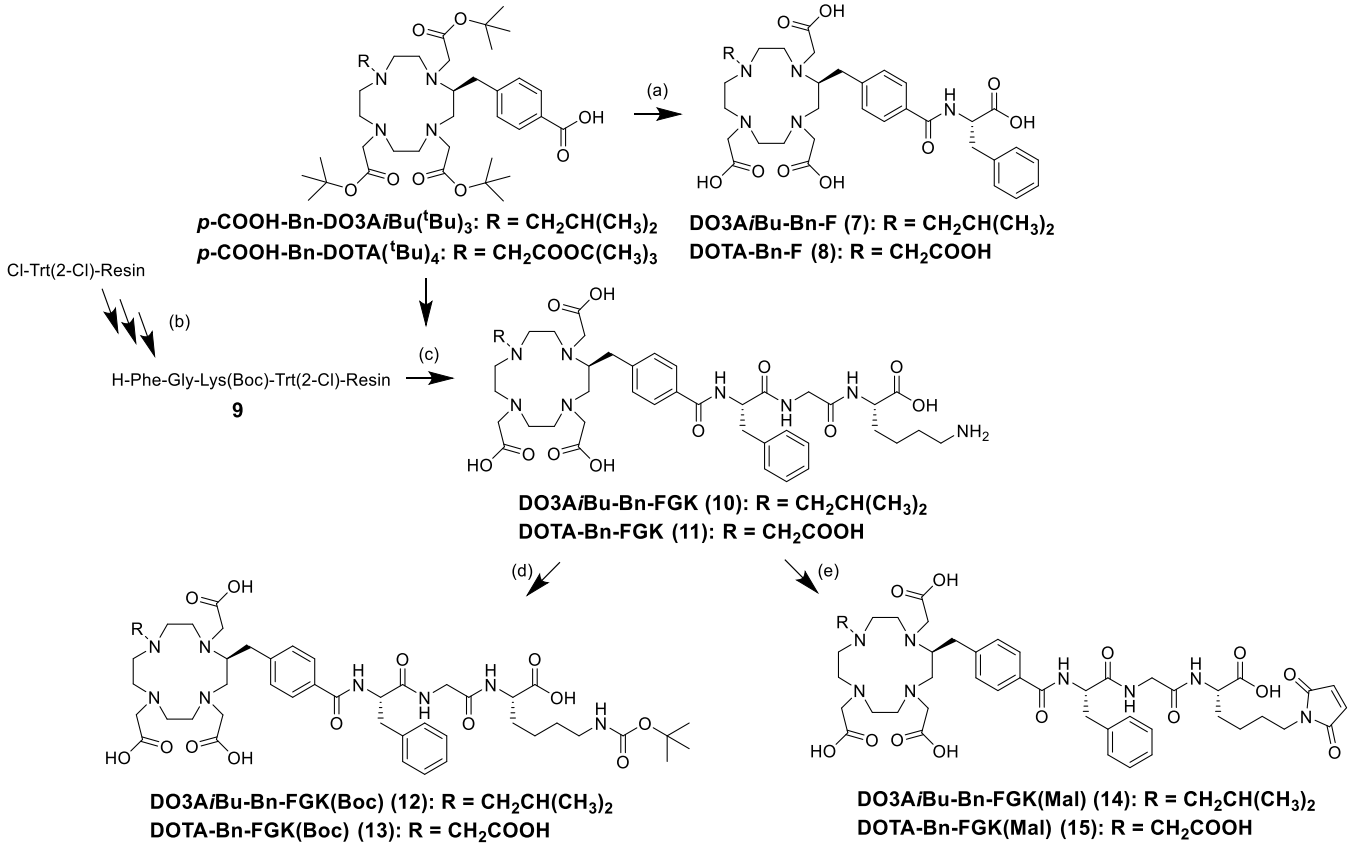

[a]Reagents and conditions: (a) (1) H-Phe-O^{t}Bu, COMU, DIEA, DMF, rt for 2 h; (2) 10% anisole/TFA, rt for 3 h, DO3A*i*Bu-Bn-F in 5.3% and DOTA-Bn-F in 14.8%; (b) (1) Fmoc-amino acids, DIC, HOBt, DMF, rt for 2 h, (2) 20% piperidine/DMF, rt for 20 min; (c) (1) DIC, HOAt, DMF, rt for 15 h, (2) TFA: triisopropylsilane: water (95/2.5/2.5), rt for 4 h, DO3A*i*Bu-Bn-FGK in 99.3% and DOTA-Bn-FGK in 52.6%; (d) $(Boc)_2O$, sat. $NaHCO_3$, dioxane, rt for 2 h, DO3A*i*Bu-Bn-FGK(Boc) in 53.8% and DOTA-Bn-FGK(Boc) in 71.8%; (e) *N*-methoxycarbonylmaleimide, sat. $NaHCO_3$, 0 °C for 2 h, DO3A*i*Bu-Bn-FGK(Mal) in 40.7% and DOTA-Bn-FGK(Mal) in 26.7%.

https://doi.org/10.1021/acs.jmedchem.3c00258
J. Med. Chem. 2023, 66, 8600−8613

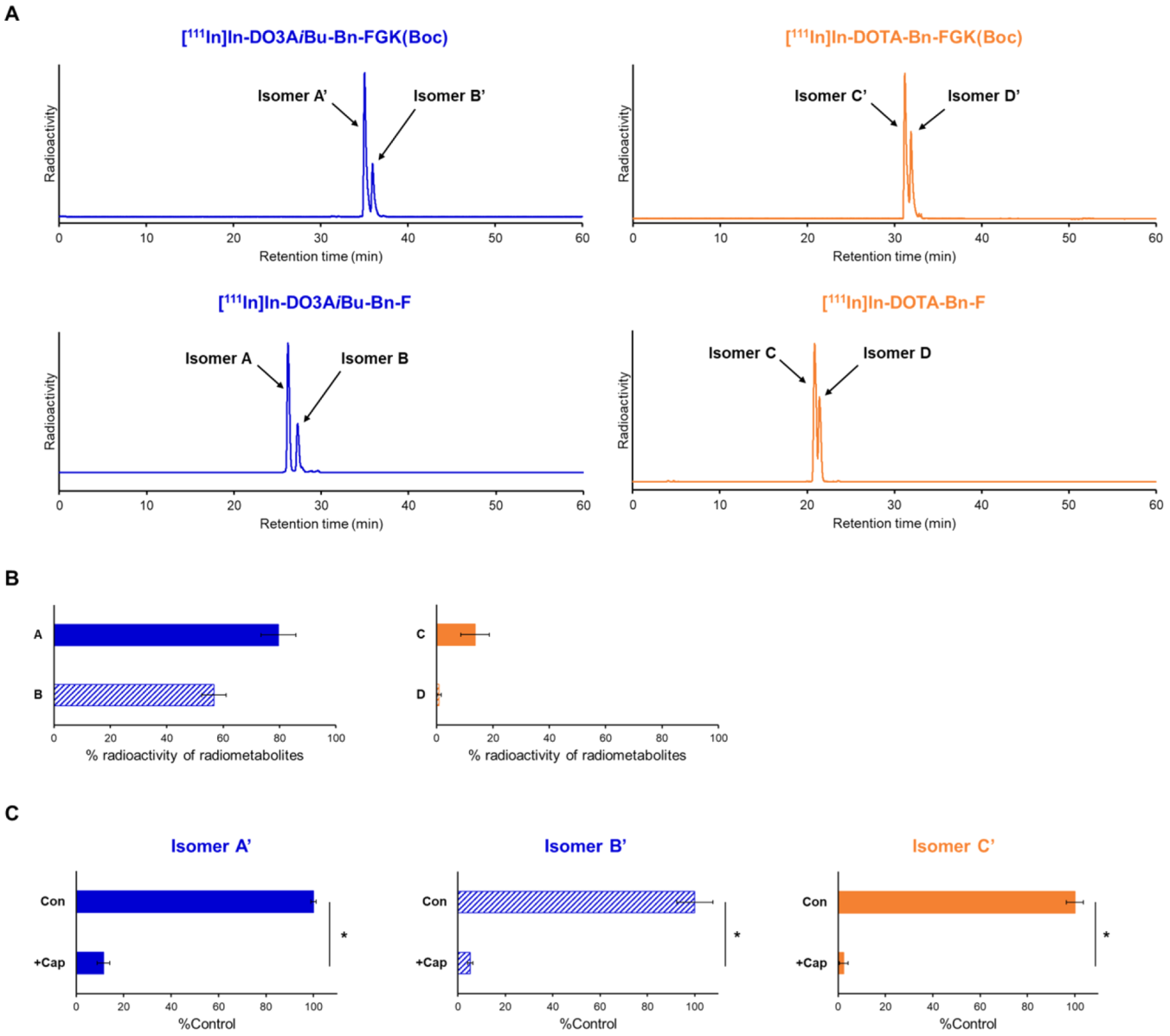

Figure 3. (A) Radiochromatograms of ^{111}In-labeled LMW substrates and the authentic radiometabolites liberated from the LMW substrates by the action of ACE on the renal BBM. Two peaks were observed for each radiochromatogram and identified as isomers by mass spectrometry of the corresponding nonradioactive In-labeled LMW substrates. (B) Liberation of radiometabolites after incubation of ^{111}In-labeled LMW substrates with BBM vesicles for 2 h. The protein concentrations of BBM vesicles were 1 mg/mL for [^{111}In]In-DO3A*i*Bu-Bn-FGK(Boc) and 10 mg/mL for [^{111}In]In-DOTA-Bn-FGK(Boc). Isomers from [^{111}In]In-DO3A*i*Bu-Bn-FGK(Boc) and [^{111}In]In-DOTA-Bn-FGK(Boc) were recognized by enzymes on the BBM vesicles to liberate the respective radiometabolite. (C) Liberation rates of radiometabolites in the absence (Con) or presence of an inhibitor for ACE, captopril (+Cap). Significances were determined by Student's *t*-test (*$p < 0.05$). The results indicated that ACE was involved in the cleavage of the FGK linkages.

and targeted radionuclide therapy using α/β^--emitters. Our previous study suggested that the physicochemical properties of radiometabolites play a crucial role in reducing renal radioactivity levels.[19] Our recent study also showed that a ^{111}In-labeled D-phenylalanine conjugated-DOTA derivative was rapidly cleared from the kidneys when liberated from a parental octreotide analogue.[21] These results suggested that [^{111}In]In-DOTA-Bn-F (Figure 1) could be a radiometabolite suitable for the renal brush border strategy.

In this study, we designed and synthesized a bifunctional chelating agent with a Phe-Gly-Lys (FGK) linkage to liberate [^{111}In]In-DOTA-Bn-F from Fab fragments by enzymes on the renal BBM, DOTA-Bn-FGK(Mal) (Figure 2). In addition, since the absence of one carboxylate in DOTA did not critically impair the stability of the resulting DO3A chelates with many trivalent ions,[22−24] another DOTA derivative, DO3A*i*Bu-Bn-FGK(Mal) (Figure 2), was also designed and synthesized to liberate a radiometabolite with physicochemical properties different from [^{111}In]In-DOTA-Bn-F (Figure 1). We used ^{111}In to represent the trivalent metallic radionuclides of clinical interest. We evaluated the enzyme recognition of the FGK linkages in ^{111}In-labeled LMW substrates ([^{111}In]In-DO3A*i*Bu-Bn-FGK(Boc) and [^{111}In]In-DOTA-Bn-FGK(Boc); Figure 1) by an *in vitro* system using renal BBM vesicles.[25] In the continuity of our prior studies, Fab fragments of a monoclonal antibody against a c-kit were used. Biodistribution studies were conducted in normal

https://doi.org/10.1021/acs.jmedchem.3c00258
J. Med. Chem. 2023, 66, 8600−8613

mice using [^{111}In]In-DOTA-Bn-SCN-Fab (Figure 2) as a reference. Besides the renal accumulation, the radioactivity in the kidney and excreted in the urine of the three ^{111}In-labeled Fabs was analyzed. The role played by the FGK linkage was also evaluated by comparing the radioactivity levels in the tumor and the kidney following injection of ^{111}In-labeled Fabs with and without the FGK linkage to nude mice bearing SY cells. From the experiments, the applicability and the future perspective of the present molecular design to radiotheranostics will be discussed.

RESULTS

Syntheses. A Bn-DOTA derivative, *p*-COOH-Bn-DOTA-(^{t}Bu)$_4$, was synthesized according to the procedure described previously.[21] Synthetic procedure for another derivative, *p*-COOH-Bn-DO3A*i*Bu(^{t}Bu)$_3$, is shown in Scheme 1. The isobutyl group was introduced to the triamide compound **1** to provide compound **2**. After reducing the amide bonds of compound **2**, the resulting cyclen derivative **3** was reacted with *tert*-butyl bromoacetate to afford compound **4**. The cross-coupling reaction and subsequent deprotection of the benzyl group afforded *p*-COOH-Bn-DO3A*i*Bu(^{t}Bu)$_3$ (**6**). Both *p*-COOH-Bn-DO3A*i*Bu(^{t}Bu)$_3$ and *p*-COOH-Bn-DOTA(^{t}Bu)$_4$ were reacted with phenylalanine *tert*-butyl ester, and subsequent deprotection produced DO3A*i*Bu-Bn-F and DOTA-Bn-F (Scheme 2) as the precursors for the authentic radiometabolites. We also synthesized DO3A*i*Bu-Bn-FG (Scheme S1) and DOTA-Bn-SCN-K (Scheme S2) to prepare authentic by-products of radiometabolites, [^{111}In]In-DO3A*i*Bu-Bn-FG and [^{111}In]In-DOTA-Bn-SCN-K (Figure 4D,E). *p*-COOH-Bn-DO3A*i*Bu(^{t}Bu)$_3$ and *p*-COOH-Bn-DOTA(^{t}Bu)$_4$ were conjugated with an FGK sequence on the resin and then cleaved from the resin with simultaneous deprotection to produce DO3A*i*Bu-Bn-FGK and DOTA-Bn-FGK (Scheme 2). Boc-reprotection of DO3A*i*Bu-Bn-FGK and DOTA-Bn-FGK afforded DO3A*i*Bu-Bn-FGK(Boc) and DOTA-Bn-FGK(Boc) (Scheme 2) used to prepare ^{111}In-labeled LMW substrates for *in vitro* studies with BBM vesicles. DO3A*i*Bu-Bn-FGK(Mal) and DOTA-Bn-FGK-(Mal) were synthesized by reacting *N*-methoxycarbonylmaleimide with the free lysine side chain of DO3A*i*Bu-Bn-FGK and DOTA-Bn-FGK (Scheme 2).

Radiolabeling of LMW Compounds with ^{111}In. Both LMW substrates, DO3A*i*Bu-Bn-FGK(Boc) and DOTA-Bn-FGK(Boc), generated two radioactive peaks on reversed-phase (RP)-HPLC upon ^{111}In complexation reactions (Figure 3A), which were identified as isomers by mass spectrometry of the corresponding nonradioactive In-labeled LMW substrates (Figure S5). Each isomer is referred to as isomers A′ and B′ for [^{111}In]In-DO3A*i*Bu-Bn-FGK(Boc) and isomers C′ and D′ for [^{111}In]In-DOTA-Bn-FGK(Boc) (Figure 3A). The authentic radiometabolites also produced isomers, which were referred to as isomers A and B for [^{111}In]In-DO3A*i*Bu-Bn-F and isomers C and D for [^{111}In]In-DOTA-Bn-F (Figure 3A). All isomers did not interconvert after isolation (Figures S2 and S5). The formation of isomers is generally observed by reacting trivalent metals with Bn-DOTA derivatives and is caused by different regiochemistry of the benzylic substitution.[21,26−28]

Log *D* Measurements. The log $D_{7.0}$ and log $D_{5.5}$ values of [^{111}In]In-DO3A*i*Bu-Bn-F and [^{111}In]In-DOTA-Bn-F were measured without separating the isomers. Although [^{111}In]In-DO3A*i*Bu-Bn-F showed higher log *D* values at both pHs than [^{111}In]In-DOTA-Bn-F, they are still highly hydrophilic with log *D* values less than −3 (Table S1).

***In Vitro* Metabolic Study.** Each isomer of ^{111}In-labeled LMW substrates was separately incubated with the BBM vesicles after RP-HPLC purification (Figure S2) to assure high radiochemical purities (>95%) and to remove large amounts of unlabeled LMW substrates (DO3A*i*Bu-Bn-FGK(Boc) or DOTA-Bn-FGK(Boc)) so that the large amounts of unlabeled substrates do not inhibit the reaction between enzymes on the BBM vesicles and tracer amounts of ^{111}In-labeled substrates. After 2 h of incubation with BBM vesicles, each isomer of ^{111}In-labeled LMW substrates generated a single radiometabolite ([^{111}In]In-DO3A*i*Bu-Bn-F or [^{111}In]In-DOTA-Bn-F) (Figure S4). [^{111}In]In-DO3A*i*Bu-Bn-FGK(Boc) was well recognized even at a protein concentration of BBM vesicles 10 times lower than that of [^{111}In]In-DOTA-Bn-FGK(Boc) (Figure 3B). The enzyme-mediated cleavage was also evaluated in the presence of inhibitor for ACE (captopril) only for isomers A′, B′, and C′ and not for D′ because the radiometabolite from isomer D′ was too small to estimate inhibition accurately (Figure S4). The enzyme-mediated cleavage of all three isomers was inhibited by captopril (Figure 3C).

Preparation of ^{111}In-Labeled Fabs. Fab fragments of a monoclonal antibody against c-kit were used as a model in the continuity of our prior studies.[16,18,19] DO3A*i*Bu-Bn-FGK(Mal) and DOTA-Bn-FGK(Mal) were conjugated with 2-iminothiolane-modified Fab using thiol-maleimide chemistry (Figure 2).[16] The numbers of DO3A*i*Bu-Bn-FGK(Mal) and DOTA-Bn-FGK(Mal) introduced per molecule of Fab were estimated to be 1.39 and 2.20, respectively, by measuring the thiol groups of the Fab before and after the conjugation reactions (1.66 to 0.27 for DO3A*i*Bu-Bn-FGK-Fab and 2.52 to 0.32 for DOTA-Bn-FGK-Fab). DOTA-Bn-SCN-Fab was also prepared as a reference by conjugating *p*-SCN-Bn-DOTA with the lysine side chain of Fab.[29] The number of *p*-SCN-Bn-DOTA molecules introduced per molecule of Fab was estimated to be 0.80 by spectrophotometric assay.[30] Radiolabeling reaction was performed for 1 h at 40 °C, and the radiochemical yields were 58.8 ± 1.0% (n = 3) for [^{111}In]In-DO3A*i*Bu-Bn-FGK-Fab, 73.0 and 69.7% (n = 2) for [^{111}In]In-DOTA-Bn-FGK-Fab, and 66.1 ± 1.4% (n = 3) for [^{111}In]In-DOTA-Bn-SCN-Fab. The chelator concentrations of DOTA-Bn-FGK-Fab and DOTA-Bn-SCN-Fab in the reaction solutions were 2.53 and 1.71 times higher than that of DO3A*i*Bu-Bn-FGK-Fab. Both DOTA-Bn-FGK-Fab and DO3A*i*Bu-Bn-FGK-Fab provided ^{111}In-labeled Fab in comparable radiochemical yields when considering the different concentrations of each chelator, indicating that the loss of one carboxylic acid in DOTA did not impair the chelating ability with ^{111}In. Since isomers in ^{111}In-labeled Fabs cannot be separated, we used the mixtures for further studies. After purification, the radiochemical purities of all ^{111}In-labeled Fabs were more than 95%, as determined by RP-TLC and SE-HPLC.

Stability and Binding Affinity of ^{111}In-Labeled Fabs. The stability of ^{111}In-labeled Fabs was evaluated both *in vitro* and *in vivo*. When ^{111}In-labeled Fabs were incubated in freshly prepared murine plasma for 24 h at 37 °C, over 97% of radioactivity remained intact as determined by RP-TLC (Table S2). The RP-TLC analyses of plasma samples obtained from murine blood at 3 h postinjection of ^{111}In-labeled Fabs showed over 95% of radioactivity remained intact (Figure S7).

The binding affinities of the three ^{111}In-labeled Fabs were determined by the competitive inhibition assay using an unmodified IgG. The IC_{50} values of the unmodified IgG were calculated from the displacement curves of radiolabeled Fabs

https://doi.org/10.1021/acs.jmedchem.3c00258
J. Med. Chem. 2023, 66, 8600−8613

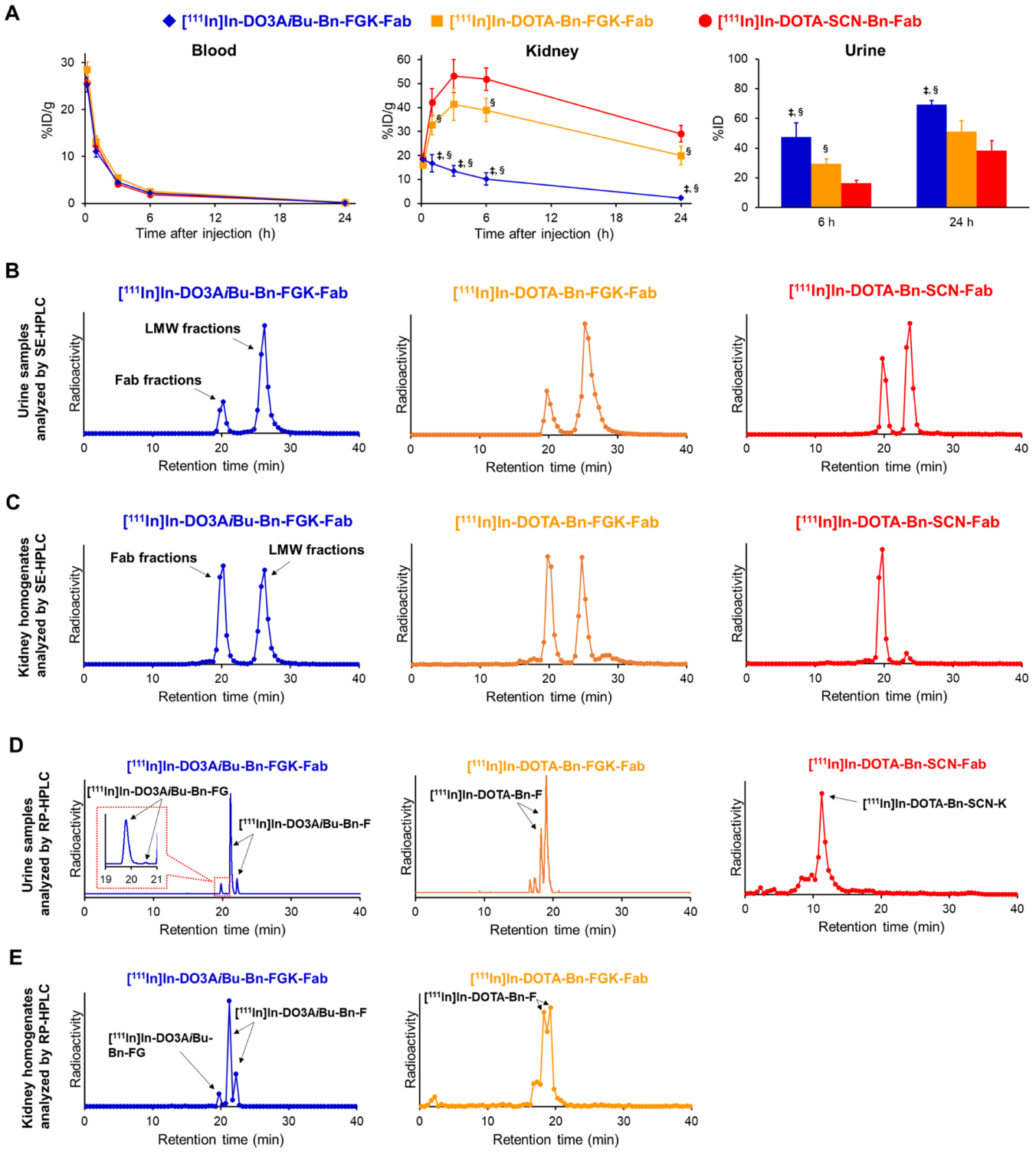

Figure 4. (A) Comparative biodistribution of radioactivity after intravenous injection of three ^{111}In-labeled Fabs in normal mice ($n = 5$). Significances were determined by one-way analysis of variance followed by Tukey's test; $p < 0.05$ compared with [^{111}In]In-DOTA-Bn-FGK-Fab (‡) and [^{111}In]In-DOTA-Bn-SCN-Fab (§). (B) SE-HPLC elution profiles of urine samples collected by 6 h injection of the three ^{111}In-labeled Fabs. (C) SE-HPLC elution profiles of kidney homogenates after 10 min injection. On SE-HPLC analyses, the intact Fabs were eluted at a retention time of around 20 min, while the radiometabolites were detected at a retention time of 22−31 min. (D) RP-HPLC elution profiles of urine samples collected by 6 h injection of three ^{111}In-labeled Fabs in normal mice. (E) RP-HPLC elution profiles of kidney homogenates after 10 min injection. The arrows indicate the radioactivity peaks of radiometabolites identified with authentic compounds.

(Figure S8). The binding affinity of c-kit IgG was not impaired for all ^{111}In-labeled Fabs.

Biodistribution in Normal Mice. All animal studies were conducted in accordance with institutional guidelines approved by the Chiba University Animal Care Committee. The biodistribution of the ^{111}In-labeled Fabs is shown in Figure 4A. Detailed results are shown in Tables S3−S5. All three ^{111}In-labeled Fabs exhibited similar radioactivity levels in the blood

https://doi.org/10.1021/acs.jmedchem.3c00258
J. Med. Chem. 2023, 66, 8600−8613

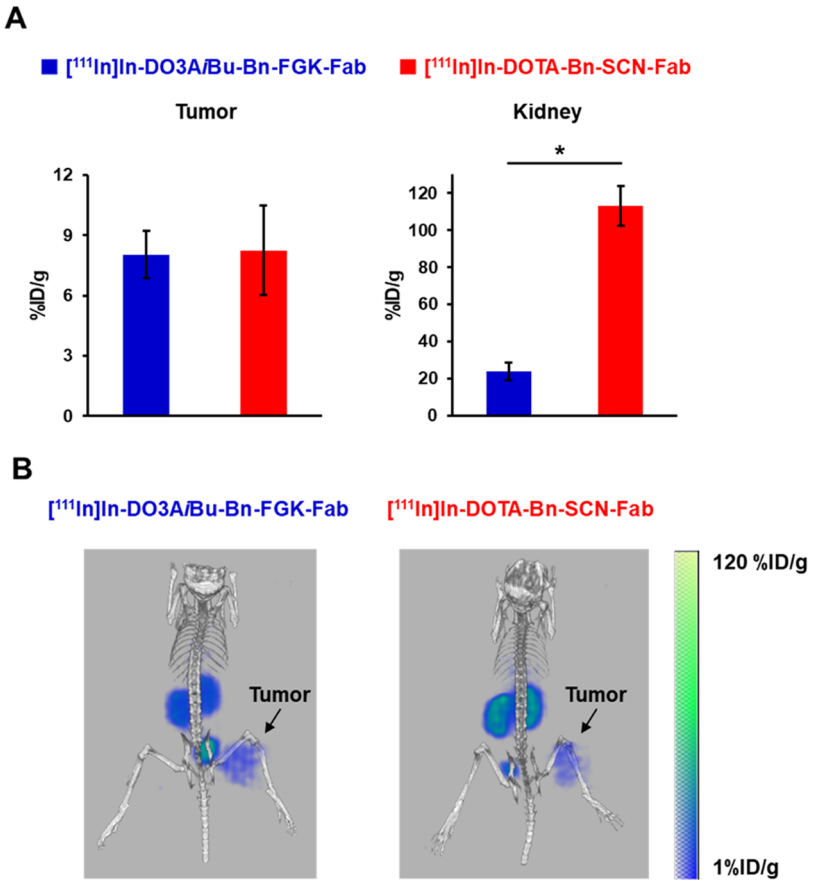

Figure 5. Biodistribution of [^{111}In]In-DO3A*i*Bu-Bn-FGK-Fab and [^{111}In]In-DOTA-Bn-SCN-Fab after injection to SY-tumor-bearing mice. (A) Radioactivity levels in the tumor and the kidney after 3 h injection ($n = 6$). Significance was determined by Student's *t*-test (*$p < 0.05$). (B) SPECT/CT images at 2.5−3.5 h postinjection of [^{111}In]In-DO3A*i*Bu-Bn-FGK-Fab and [^{111}In]In-DOTA-Bn-SCN-Fab.

from 10 min to 24 h postinjection in normal mice. However, marked differences were observed in the renal radioactivity levels. While [^{111}In]In-DOTA-Bn-FGK-Fab showed lower renal radioactivity levels than [^{111}In]In-DOTA-Bn-SCN-Fab at 1, 6, and 24 h postinjection, [^{111}In]In-DO3A*i*Bu-Bn-FGK-Fab showed significantly lower renal radioactivity levels from 1 to 24 h postinjection than [^{111}In]In-DOTA-Bn-FGK-Fab. Significant differences were also observed in the radioactivity levels of the urine collected for 6 h after administration of [^{111}In]In-DO3A*i*Bu-Bn-FGK-Fab and [^{111}In] In-DOTA-Bn-SCN-Fab ($p < 0.05$) as well as between [^{111}In]In-DOTA-Bn-FGK-Fab and [^{111}In]In-DOTA-Bn-SCN-Fab ($p < 0.05$).

Metabolic Studies in Normal Mice. The SE-HPLC analyses of the urine samples showed that [^{111}In]In-DO3A*i*Bu-Bn-FGK-Fab and [^{111}In]In-DOTA-Bn-FGK-Fab excreted higher amounts of LMW fractions than [^{111}In]In-DOTA-Bn-SCN-Fab (Figure 4B). The LMW fractions in the urine samples were subjected to ultrafiltration and analyzed by RP-HPLC. The LMW fractions from [^{111}In]In-DO3A*i*Bu-Bn-FGK-Fab, [^{111}In]In-DOTA-Bn-FGK-Fab, and [^{111}In]In-DOTA-Bn-SCN-Fab were mainly eluted at a retention time identical to that of [^{111}In]In-DO3A*i*Bu-Bn-F, [^{111}In]In-DOTA-Bn-F, and [^{111}In]In-DOTA-Bn-SCN-K, respectively (Figure 4D). The other radiometabolite observed with the metabolic analysis of [^{111}In]In-DO3A*i*Bu-Bn-FGK-Fab was identified as [^{111}In]In-DO3A*i*Bu-Bn-FG (19.8 and 20.6 min of retention time). Although one isomer was observed as only a slight peak (20.6 min of retention time), the liberation of both isomers was confirmed. The radioactivity in the kidney 10 min postinjection of ^{111}In-labeled Fabs was also analyzed using the same analytical methods. The SE-HPLC analysis showed that the radioactivity at the LMW fractions (22−31 min) was 10.9 ± 4.3% ($n = 3$) of total applied radioactivity for [^{111}In]In-DOTA-Bn-SCN-Fab (Figure 4C). On the other hand, both [^{111}In]In-DO3A*i*Bu-Bn-FGK-Fab and [^{111}In]In-DOTA-Bn-FGK-Fab generated LMW fractions similar to each other (50.4 ± 8.6% ($n = 3$) for the former and 53.7 and 47.3% ($n = 2$) for the latter) and much higher than [^{111}In]In-DOTA-Bn-SCN-Fab (Figure 4C). The RP-HPLC analysis of the LMW fractions of [^{111}In]In-DO3A*i*Bu-Bn-FGK-Fab and [^{111}In]In-DOTA-Bn-FGK-Fab showed that radioactivity was mainly eluted at a retention time identical to that of [^{111}In]In-DO3A*i*Bu-Bn-F and [^{111}In]In-DOTA-Bn-F, respectively (Figure 4E). The isomers A and B of [^{111}In]In-DO3A*i*Bu-Bn-F were detected in the kidney and the urine after injection of [^{111}In]In-DO3A*i*Bu-Bn-FGK-Fab (Figure 4D,E). Similarly, [^{111}In]In-DOTA-Bn-FGK-Fab provided the isomers C and D of [^{111}In]In-DOTA-Bn-F in the kidney and the urine (Figure 4D,E). These results indicate that each pair of isomers was excreted from the kidney into the urine, satisfying the prerequisites for a radiometabolite in the current molecular design. The radioactivity in the LMW fractions of [^{111}In]In-DOTA-Bn-SCN-Fab was too low to be analyzed by RP-HPLC.

Biodistribution in Tumor-Bearing Mice. No significant difference was observed in the radioactivity levels in tumors between [^{111}In]In-DO3A*i*Bu-Bn-FGK-Fab and [^{111}In]In-

https://doi.org/10.1021/acs.jmedchem.3c00258
J. Med. Chem. 2023, 66, 8600−8613

DOTA-Bn-SCN-Fab. However, [^{111}In]In-DO3A*i*Bu-Bn-FGK-Fab exhibited significantly lower renal radioactivity levels than [^{111}In]In-DOTA-Bn-SCN-Fab (Figure 5A and Table S6) ($p < 0.05$). The SPECT images clearly reflected the lower renal radioactivity levels of [^{111}In]In-DO3A*i*Bu-Bn-FGK-Fab in the kidney than those of [^{111}In]In-DOTA-Bn-SCN-Fab (Figure 5B).

DISCUSSION

For successful reduction of the renal radioactivity shortly after injection of radiolabeled LMW Abs, both discriminated cleavage of the linkage at the renal BBM and subsequent release of a urinary excretable radiometabolite are the two indispensable requisites. Considering our prior study,[18] we selected a tripeptide sequence with *N*-terminus Phe and C-terminus Lys, F-X-K, so that the F-X bond is cleaved with dipeptidyl carboxypeptidases on the renal BBM. Since the *C*-terminus free carboxylate would be crucial for enzyme recognition by dipeptidyl carboxypeptidases, the ε-amino group of lysine was converted to a maleimide group for antibody conjugation while remaining a free carboxylate. We then searched for enzymes on BBM that recognize the F-X-G sequence with angiotensin-converting enzyme (ACE) being one candidate as it cleaves the F-G bond in the FGG sequence from the *C*-terminus of its substrates.[31] ACE recognizes the FGG sequence even when a furanacryloyl group is introduced to the *N*-terminus-Phe-Gly-Gly.[32] Thus, the respective DOTA derivatives were conjugated to the *N*-terminus of the FGK tripeptide, and the ε-amino group of Lys was converted to maleimide to prepare DO3A*i*Bu-Bn-FGK(Mal) and DOTA-Bn-FGK(Mal) (Figure 2).

Due to the presence of ACE in plasma and in the surface of endothelial and epithelial cells,[33] the ^{111}In-labeled Fabs modified with FGK linkages could be amenable to premature cleavage in the blood circulation, which would impair the tumor accumulation. Three experiments were conducted to evaluate the stability of the linkage in ^{111}In-labeled Fabs. First, the three ^{111}In-labeled Fabs were incubated in freshly prepared murine plasma for 24 h, and over 97% of the radioactivity was observed in the Fab fractions (Table S2). The murine plasma samples obtained from the blood 3 h after injection of the three ^{111}In-labeled Fabs were analyzed, and found that more than 95% of the radioactivity remained stable (Figure S7). The radioactivity levels in the blood were also compared after injection of the three ^{111}In-labeled Fabs into mice. The two radiometabolites, [^{111}In]In-DOTA-Bn-F and [^{111}In]In-DO3A*i*Bu-Bn-F, exhibited rapid elimination rates from the blood upon intravenous injection (Tables S7 and S8). Thus, if the FGK linkage is cleaved in the blood, the radioactivity levels of ^{111}In-labeled Fabs with the FGK linkage in the blood should be lower than those of [^{111}In]In-DOTA-Bn-SCN-Fab. The three ^{111}In-labeled Fabs exhibited similar radioactivity levels in the blood, as shown in Figure 4A and Tables S3−S5. These findings confirmed that the FGK linkage in the two ^{111}In-labeled Fabs remained stable in the blood. In our prior studies of ester bonds as the cleavable linkage, the ester bond exhibited higher stability when conjugated to IgG antibody than to Fab, although both exhibited similar stability in a buffered-solution at pH 7.4.[34] Similarly, an ester bond introduced proximal to an IgG molecule using exposed thiol groups showed much higher stability than an ester bond introduced distal from an IgG molecule (2-iminothiolane modification).[35] The cleavable GFK linkage also remained stable in plasma when [^{99m}Tc]Tc-IPG-GFK was conjugated with Fabs.[18] Thus, the steric hindrance induced by Fab molecules plays a crucial role in the stability of cleavable linkages in the blood.

After the ^{111}In-labeling reaction, ^{111}In-labeled Fabs consist of tracer amounts of ^{111}In-labeled Fabs and large amounts of unlabeled Fabs. As a result, unlabeled Fabs compete for the enzymatic reaction on the BBM vesicles with ^{111}In-labeled Fabs. Furthermore, the positively charged unlabeled Fabs may exhibit electrostatic interaction with the negatively charged surface of the BBM vesicle, which hinders the access of ^{111}In-labeled Fabs to the enzymes. Removing unlabeled Fabs from ^{111}In-labeled Fabs is difficult to achieve in a simple procedure. Thus, after RP-HPLC purification, [^{111}In]In-DOTA-Bn-FGK(Boc) and [^{111}In]In-DO3A*i*Bu-Bn-FGK(Boc) were incubated with BBM vesicles to estimate the enzyme-mediated release of radiometabolites. [^{111}In]In-DO3A*i*Bu-Bn-FGK(Boc) released much higher amounts of radiometabolites than [^{111}In]In-DOTA-Bn-FGK(Boc) (Figure 3B). The *N*-isobutylation of DOTA neutralizes the net charge of the In-DO3A*i*Bu complex and provides a partial lipophilic group. Such properties of tracer amounts of [^{111}In]In-DO3A*i*Bu-Bn-FGK(Boc) may have facilitated the access of the substrate to ACE on the BBM vesicles. The electrostatic repulsion between the negatively charged [^{111}In]In-DOTA-Bn-FGK(Boc) and the negatively charged BBM vesicle surface would have also hindered access to the enzyme on the BBM vesicles. Similar results were observed in our prior study.[17] The marked reduction in the radiometabolites formation by the presence of captopril indicates the involvement of ACE in cleaving the FGK linkage (Figure 3C).

For the biodistribution studies in normal mice, ^{111}In-labeled Fabs with similar mass and radioactivity were injected into mice. Since all ^{111}In-labeled Fabs remained stable in the blood (Table S2 and Figure S7), similar mass amounts and radioactive portions of the three ^{111}In-labeled Fabs would be filtered by the glomerulus and reach the proximal tubular epithelial cells of the kidney. Indeed, the three ^{111}In-labeled Fabs registered similar renal radioactivity levels at 10 min postinjection. However, significant differences were observed in the renal radioactivity levels among the three after that time point (Figure 4A, Tables S3−S5). Both ^{111}In-labeled Fabs with the FGK linkage significantly lowered the renal radioactivity levels than [^{111}In]In-DOTA-Bn-SCN-Fab. When [^{111}In]In-DOTA-Bn-FGK-Fab and [^{111}In]In-DOTA-Bn-SCN-Fab are compared, both registered the maximum renal radioactivity levels at 3 h postinjection, followed by a gradual decrease. Contrary to [^{111}In]In-DOTA-Bn-FGK-Fab, [^{111}In]In-DO3A*i*Bu-Bn-FGK-Fab showed the maximum renal radioactivity levels at 10 min postinjection, followed by a decrease with time (Figure 4A). Since both ^{111}In-labeled Fabs with the FGK linkage generated similar amounts of their final metabolites at 10 min postinjection (Figure 4C,E), the different renal radioactivity levels between the two after the postinjection time would be caused by faster elimination rate of [^{111}In]In-DO3A*i*Bu-Bn-F than that of [^{111}In]In-DOTA-Bn-F from coated vesicles of the kidney.[19] Although [^{111}In]In-DO3A*i*Bu-Bn-F possesses higher lipophilicity than [^{111}In]In-DOTA-Bn-F, as observed in the longer retention times on the RP-HPLC (Figure S5) and higher log *D* values, the log *D* values of the former were less than −3 (Table S1). Thus, the passive diffusion rates of [^{111}In]In-DO3A*i*Bu-Bn-F would not account for the faster elimination rates from the kidney. Some unknown mechanisms that favor a net neutral charge with a partial lipophilic isobutyl group may be involved. Contrary to *in vitro* results with BBM vesicles (Figure 3B), the

https://doi.org/10.1021/acs.jmedchem.3c00258
J. Med. Chem. 2023, 66, 8600−8613

two ^{111}In-labeled Fabs with the FGK linkage generated similar amounts of radiometabolites at 10 min postinjection (Figure 4C). Similar phenomena were observed in our prior studies with [^{188}Re]Re-CpTR-GK-Fab, [^{99m}Tc]Tc-MAG$_3$-GFK-Fab, and [^{64}Cu]Cu-NOTA-MVK-Fab.[15,17,19] While these radiolabeled Fabs showed low renal radioactivity levels shortly after injection into mice due to the excretion of the radiometabolites, their corresponding LMW substrates hardly generated their metabolites when incubated with BBM vesicles. Although species differences may partially be involved (BBM vesicles are isolated from rat kidneys), the *in vitro* system may have underestimated the cleavage rates due to the physicochemical properties of the LMW substrates. However, the different physicochemical properties of each substrate would become of minor influence when attached to macromolecules.

Brandt et al. recently suggested that once the protein enters the proximal tubule, it appears likely that other proteases, e.g., meprin A, predigest the radiolabeled protein resulting in the formation of at least one radiolabeled fragment whose size now enables the action of NEP.[36] Our earlier study showed that a small amount of LMW radiolabeled species was observed in the kidney at 10 and 30 min postinjection of directly radioiodinated Fabs.[37] Similarly, a small amount of LMW ^{111}In-labeled species was observed at 10 min postinjection of [^{111}In]In-DOTA-Bn-SCN-Fab (Figure 4C). While the formation of such LMW radiolabeled species would lead to the generation of the designed radiometabolites (radioiodinated hippuric acid for HML-Fab, and [^{111}In]In-DOTA-Bn-F or [^{111}In]In-DO3A*i*Bu-Bn-F for the present study), another mechanism is needed to account for the low renal radioactivity levels at early postinjection times. In this context, as mentioned before for the esterase-mediated cleavage of the ester bonds in radiolabeled antibodies, the esterase acts only when the ester bonds are less sterically hindered within the antibody molecules.[35] Accordingly, it appears likely that some peptide bonds in the ^{111}In-labeled Fabs would be cleaved nonspecifically by enzymes on the renal BBM, which would decrease the steric hindrance of antibody molecules and facilitate the access of ACE to the FGK linkage to liberate the radiometabolite. The statement mentioned above would account for the potential mechanism for the renal metabolism of radiolabeled Fabs with a cleavable linkage and the discrepancy between the *in vitro* studies with BBM vesicles and *in vivo* studies in mice. Our earlier study showed that when radioiodinated HML ([*I]HML) was conjugated to Fabs using thiol groups generated by reducing the interchain disulfide bonds of Fabs, [*I]HML-Fab generated higher amounts of radiometabolites of a variety of molecular sizes in the kidney at 10 min postinjection. However, [*I]hippuric acid was the only radiometabolite when [*I]HML was conjugated to 2-iminothiolane-modified Fabs.[37] The reduction of some disulfide bonds in Fab molecules and subsequent alkylation of the thiol groups may have induced partial changes in their structures, which would promote the nonspecific digestion of peptide bonds in the Fab molecules by a variety of enzymes on the BBM. Thus, the antibody modification may constitute an approach to accelerate the generation of radiometabolites in the kidney.

The ability of [^{111}In]In-DO3A*i*Bu-Bn-FGK-Fab to reduce the renal radioactivity levels without impairing the radioactivity levels in the tumor was demonstrated by the biodistribution and the SPECT images in SY-tumor-bearing mice (Figure 5). These findings indicate that DO3A*i*Bu-Bn-FGK(Mal) would be useful for preparing ^{111}In-labeled LMW Abs with low renal radioactivity levels. Reducing renal radioactivity levels of radiolabeled LMW Abs is also needed for radioimmunotherapy to decrease renal toxicity. Although further studies are needed to apply DO3A*i*Bu-Bn-FGK(Mal) to therapeutic radionuclides such as ^{90}Y, ^{177}Lu, and ^{225}Ac, the findings in this study would provide fundamental knowledge for future applications of a DOTA-based radiotheranostic platform for LMW Abs. Radiolabeled peptides also exhibit high and persistent radioactivity levels in the kidney, which causes dose-limiting nephrotoxicity.[38] Since LMW Abs and peptides share similar metabolic pathways in the kidney,[11] the renal brush border strategy was recently applied to peptides.[36,39,40] For the applications, further efforts may be needed to stabilize the cleavable linkage in the blood while liberating a urinary excretable radiometabolite at the renal brush border.

CONCLUSIONS

We developed a DOTA-based bifunctional chelating agent with a cleavable linkage to prepare ^{111}In-labeled Fabs with low renal radioactivity levels. In this design, contrary to our previous studies using substrates for NEP as the cleavable linkage, we employed an FGK linkage to liberate a urinary excretable [^{111}In]In-DO3A*i*Bu-Bn-F from ^{111}In-labled Fabs by the action of ACE. The findings in this study indicate that an appropriate enzyme can be used from many kinds of enzymes on the renal BBM to liberate a designed urinary excretable radiometabolite from LMW Abs. The present study also confirms the significant role played by radiometabolites in reducing renal radioactivity levels. In addition, the involvement of nontarget enzymes was suggested for liberating the radiometabolites from parental antibodies. These findings provide a good basis for future applications of a DOTA-based radiotheranostic platform for LMW Abs.

EXPERIMENTAL SECTION

General. ^{1}H NMR spectra were recorded on a JEOL JNM-ECS 400 spectrometer (JEOL). Mass spectrometry was performed using an AccuTOF LC-plus (JMS-T100LP, JEOL). Analytical reversed-phase (RP)-HPLC was performed with a Unison US-C18 column (4.6 mm × 150 mm, Imtakt) at a flow rate of 1.0 mL/min with a linear gradient starting from 100% A (0.1% aqueous trifluoroacetic acid (TFA)) and 0% B (acetonitrile with 0.1% TFA) to 45% B at 30 min, and then to 100% B at 35 min (system A), or from 0% B to 15% B at 30 min, and then to 100% B at 35 min (system B), or 30% B to 100% B at 20 min (system C), or with two Unison US-C18 columns (4.6 mm × 150 mm, Imtakt) connected in series at a flow rate of 1.0 mL/min with a linear gradient starting from 100% A (0.05 M ammonium acetate) 0% B (acetonitrile) to 50% B at 50 min, and then to 100% B at 55 min (System D). Preparative RP-HPLC was performed on a Cadenza 5CD-C18 column (20 mm × 150 mm, Imtakt) at a flow rate of 5.0 mL/min with a linear gradient starting from 100% A (0.1% aqueous TFA) and 0% B (acetonitrile with 0.1% TFA) to 60% B at 30 min, and then to 100% B at 35 min (system E), or from 0% B to 45% B at 30 min, and then to 100% B at 35 min (system F), or from 5% B to 50% B at 35 min, and then to 100% B at 45 min (system G), or from 5% B to 30% B at 35 min, and then to 100% B at 40 min (system H), or from 0% B to 60% B at 40 min, and then to 100% B at 45 min (system I), or from 0% B for 5 min, to 60% B at 35 min, and then to 100% B at 40 min (system J), or from 0% B for 5 min, to 45% B at 35 min, and then to 100% B at 50 min (system K). Size exclusion (SE)-HPLC was performed with a Cosmosil Diol-300-II column (7.5 mm ID × 600 mm, Nacalai Tesque) at a flow rate of 1 mL/min with 0.1 M phosphate buffer (pH 6.8). The effluent was monitored by detection at 254 nm with a UV detector (L-7405, Hitachi) coupled to a NaI(Tl) radioactivity detector (Gabi star, Raytest), or collected with a fraction collector (Frac-920, GE Healthcare) at 0.5 min intervals, and the radioactivity counts in each

https://doi.org/10.1021/acs.jmedchem.3c00258
J. Med. Chem. 2023, 66, 8600−8613

fraction were determined with an auto-well gamma counter (Wizard 3, PerkinElmer Japan). RP-TLC (Silica gel 60 RP-18 F254S, Merck) was developed with a mixture of 10% aqueous ammonium acetate and MeOH with (2:3, v/v). The RP-TLC was cut into 5 mm fractions, and the radioactivity was measured with an auto-well gamma counter (Wizard 3). The compounds **1** and *p*-COOH-Bn-DOTA(^{t}Bu)$_4$ were prepared by the same procedure described previously.[21] Chemicals purchased from commercial sources were of reagent grade or higher and used without further purification. A centrifuged column procedure using Sephadex G-50 fine (GE Healthcare) was performed as follows. A centrifuged column was prepared by adding Sephadex G-50 fine (GE Healthcare) gel in each buffer into a Mobicol column (MoBiTec) and equilibrated by centrifuge at 400*g* for 2 min. Each 100 μL of Fab solution was applied and centrifuged at 400*g* for 2 min to provide the purified Fab solution as the eluent. $^{111}InCl_3$ (74 MBq/mL) was purchased from Nihon Medi-Physics. Male Wistar rats, ddY mice, and BALB/c-nu/nu mice were obtained from Japan SLC. Chemicals purchased from commercial sources were of reagent grade or higher and used without further purification. The chemical purities of key intermediate (**6**) and precursors used for radiolabeling reactions were determined by RP-HPLC analyses and were found to be >95% (Figure S1). Radiochemical purities of radiolabeled compounds used for *in vitro* or *in vivo* studies were determined by RP-TLC and RP-HPLC and were >97% for both analyses (Figures S2 and S3).

Monoclonal Antibody and Cells. The monoclonal antibody against c-kit (12A8) and non-small-cell lung cancer SY cells expressing high c-kit levels,[41,42] were obtained from Immuno-Biological Laboratories (Takasaki, Japan). C-kit is overexpressed in several human tumors including small-cell lung carcinomas and gastrointestinal stromal tumors.[43,44] The Fabs of 12A8 were prepared using the Fab Preparation Kit (Pierce). SY cells were cultivated in RPMI-1640 medium (Nacalai Tesque) supplemented with 10% fetal bovine serum (Thermo Scientific) in a humidified atmosphere containing 5% carbon dioxide at 37 °C. The cells were grown to 80 to 90% confluence before trypsinization and formulation into an equal volume of RPMI-1640 medium and Matrigel (BD Biosciences) for implantation into mice.

Syntheses. *Synthesis of p-COOH-Bn-DO3AiBu(^{t}Bu)$_3$. (S)-5-(p-Iodobenzyl)-1-isobutyl-3,6,11-trioxo-1,4,7,10-tetraazacyclododecane (**2**).* To a suspension of compound **1** (913 mg, 1.96 mmol) and sodium triacetoxyborohydride (498 mg, 1.2 equiv) in THF (20 mL) was added isobutyraldehyde (357 μL, 2 equiv) under argon atmosphere. After the mixture was stirred for 24 h at room temperature, water (20 mL) was added. After removing THF *in vacuo*, the resulting aqueous solution was extracted from chloroform (10 mL × 3) and dried over anhydrous Na_2SO_4. After removing the solvent *in vacuo*, the residue was subjected to flash chromatography on silica gel using a mixture of chloroform/methanol (starting from 100:0 to 90:10) as an eluent to provide **2** as a white solid (403 mg, 0.829 mmol, 42.4%). ^{1}H NMR ($CDCl_3$): δ 0.91 −0.96 [6H, m, CH_3], 1.66−1.76 [1H, m, CH], 2.36−2.48 [2H, m, CH_2], 2.79−2.85 [1H, m, CH_2], 3.02−3.32 [5H, m, CH_2], 3.47 [2H, d, J = 5.2 Hz, CH_2], 3.61−3.74 [2H, m, CH_2], 4.61 [1H, dd, J = 16.8 and 8.0 Hz, CH], 6.47 [1H, s, NH], 6.61 [1H, s, NH], 6.94−6.99 [3H, overlapped, CH, NH], 7.57 [2H, d, J = 8.0 Hz, CH]. HR-MS(ESI) calcd for $C_{19}H_{28}IN_4O_3$ [M + H]$^+$: m/z 487.12061, found 487.12041.

*(S)-5-(p-Iodobenzyl)-1-isobutyl-1,4,7,10-tetraazacyclododecane (**3**).* To a chilled (0 °C) suspension of **2** (403 mg, 0.829 mmol) in THF (4 mL) was added 0.95 M BH_3-THF/THF solution (14 mL, 16 equiv) under argon atmosphere. The mixture was stirred for 1 h at 0 °C and then heated to reflux for 24 h. The solution was cooled to 0 °C, quenched with methanol (20 mL) for 1 h, and then evaporated to dryness. The residue was dissolved in methanol (20 mL) again, and the solvent was evaporated. The residue was then dissolved in conc. HCl (20 mL), and the solution was stirred for 24 h at room temperature. After the solution was cooled to 0 °C, 12.5 *N* aq. NaOH was added to basify and extracted with chloroform (20 mL × 3). The combined organic phases were dried over anhydrous $MgSO_4$, and the solvent was removed *in vacuo*. The residue was subjected to flash chromatography on silica gel using a mixture of chloroform/methanol/25% NH_3 aqueous solution (100:10:1) as an eluent to provide **3** as a yellow oil (275 mg, 0.619 mmol, 74.7%). ^{1}H NMR (CD_3OD): δ 0.81−0.86 [6H, m, CH_3], 1.71−1.80 [1H, m, CH], 2.00−2.81 [19H, m, CH, CH_2], 6.87 [2H, d, J = 8.4 Hz, CH], 7.58−7.60 [2H, d, J = 8.0 Hz, CH]. HR-MS(ESI) calcd for $C_{19}H_{34}IN_4$ [M + H]$^+$: m/z 445.18282, found 445.18299.

*Tris(tert-Butyl) (S)-5-(p-Iodobenzyl)-1-isobutyl-1,4,7,10-tetraazacyclododecane-4,7,10-triacetate (**4**).* To a chilled suspension (0 °C) of **3** (275 mg, 0.619 mmol) and Na_2CO_3 (295 mg, 4.5 equiv) in a solution of acetonitrile (5 mL) was added *tert*-butyl bromoacetate (0.41 mL, 4.5 equiv) under argon atmosphere. After the addition, the mixture was heated to reflux for 24 h, and the filtrate was evaporated *in vacuo*. The residue was dissolved in a saturated $NaHCO_3$ solution (5 mL) and extracted with chloroform (10 mL × 3). The combined organic phases were dried over anhydrous $MgSO_4$, and the solvent was removed *in vacuo*. The residue was subjected to flash chromatography on silica gel using a mixture of chloroform/methanol (starting from 100:0 to 80:20) as an eluent to provide **4** as a yellow oil (286 mg, 0.364 mmol, 58.8%). ^{1}H NMR ($CDCl_3$): δ 0.80−1.07 [6H, m, CH_3], 1.20−1.44 [27H, overlapped, ^{t}Bu], 2.09−2.18 [1H, m, CH], 2.47−3.75 [25H, overlapped, CH, CH_2, *DOTA*], 6.97 [2H, d, J = 7.6 Hz, CH], 7.55 [2H, d, J = 7.6 Hz, CH]. HR-MS(ESI) calcd for $C_{37}H_{64}IN_4O_6$ [M + H]$^+$: m/z 787.38705, found 787.38926.

*Tris(tert-Butyl) (S)-5-(p-Benzyloxycarbonylbenzyl)-1-isobutyl-1,4,7,10-tetraazacyclododecane-4,7,10-triacetate (**5**).* A mixed solution of **4** (286 mg, 0.364 mmol), $Pd(OAc)_2$ (8.2 mg, 0.1 equiv), 1,2-bis(diphenylphosphino)ethane (21.7 mg, 0.15 equiv), TEA (152 μL, 3 equiv), and benzyl alcohol (753 μL, 20 equiv) in DMF (2.5 mL) was heated to 80 °C for 24 h under carbon monoxide atmosphere. The solvent was removed *in vacuo*, and the residue was suspended in ethyl acetate (10 mL). After the mixture was filtered, the filtrate was washed with 5% $NaHCO_3$ (5 mL × 3) and dried over anhydrous $MgSO_4$. After removing the solvent *in vacuo*, the residue was subjected to flash chromatography on silica gel using a mixture of chloroform/methanol (starting from 100:0 to 80:20) as an eluent to provide **5** as a yellow oil (73.8 mg, 92.8 μmol, 25.5%). ^{1}H NMR ($CDCl_3$): δ 1.07 [6H, t, J = 6.2 Hz, CH_3], 1.18−1.54 [27H, overlapped, ^{t}Bu], 2.08−3.65 [26H, overlapped, CH, CH_2, *DOTA*], 5.33 [2H, s, CH_2], 7.28−7.43 [7H, overlapped, CH], 7.97 [2H, d, J = 8.0 Hz, CH]. HR-MS(ESI) calcd for $C_{45}H_{71}N_4O_8$ [M + H]$^+$: m/z 795.52719, found 795.53072.

*Tris(tert-Butyl) (S)-5-(p-Hydroxycarbonylbenzyl)-1-isobutyl-1,4,7,10-tetraazacyclododecane-4,7,10-triacetate (p-COOH-Bn-DO3AiBu(^{t}Bu)$_3$) (**6**).* To a solution of **5** (73.8 mg, 92.8 μmol) in methanol (1.0 mL) was added 10% Pd/C (200 mg) and stirred for 5 h under H_2 atmosphere. After filtration, the solvent was evaporated *in vacuo* to provide *p*-COOH-Bn-DO3AiBu(^{t}Bu)$_3$ as a white solid (31.9 mg, 45.3 μmol, 48.8%). ^{1}H NMR ($CDCl_3$): δ 0.85−0.89 [6H, m, CH_3], 1.36−1.51 [27H, overlapped, ^{t}Bu], 1.87−3.78 [26H, overlapped, CH, CH_2, *DOTA*], 7.20−7.24 [2H, m, CH], 7.97−8.22 [2H, m, CH]. HR-MS(ESI) calcd for $C_{38}H_{65}N_4O_8$ [M + H]$^+$: m/z 705.48024, found 705.48196. HPLC purity >99%, retention time 9.4 min (system C).

*Synthesis of Phe Adducts of the Chelators. DO3AiBu-Bn-F (**7**).* To a solution of *p*-COOH-Bn-DO3AiBu(^{t}Bu)$_3$ (2.7 mg, 3.83 μmol) in DMF (0.4 mL) were added L-phenylalanine *tert*-butyl ester hydrochloride (1.5 mg, 1.5 equiv), *N*,*N*-diisopropylethylamine (DIEA, 2.9 μL, 4.5 equiv), and {{[(1-cyano-2-ethoxy-2-oxoethylidene)amino]-oxy}-4-morpholinomethylene} dimethylammonium hexafluorophosphate (COMU, 4.9 mg, 3.0 equiv), successively. After stirring for 2 h at room temperature, the solvent was removed *in vacuo*. The residue was dissolved in ethyl acetate, washed with 5% $NaHCO_3$ (5 mL × 3) and 5% citric acid (5 mL × 3) successively, and dried over anhydrous Na_2SO_4. After the solvent was removed *in vacuo*, the residue was dissolved in 10% anisole/TFA (2.0 mL) and stirred for 3 h at room temperature. After the solvent was removed *in vacuo*, diethyl ether (2.0 mL) was added to the residue to give the precipitate. The precipitate was purified by preparative RP-HPLC (system E, 25.0 min of retention time) to provide DO3AiBu-Bn-F as a white solid (0.2 mg, 0.203 μmol, 5.3%). HR-MS(ESI) calcd for $C_{35}H_{48}N_5O_9$ [M − H]$^-$: m/z 682.34520, found 682.34899. HPLC purity 96.3%, retention time 22.1 min (system A).

https://doi.org/10.1021/acs.jmedchem.3c00258
J. Med. Chem. 2023, 66, 8600−8613

*DOTA-Bn-F (**8**).* DOTA-Bn-F was prepared according to the same procedure as DO3A*i*Bu-Bn-F using *p*-COOH-Bn-DOTA(^{t}Bu)$_4$ (4.5 mg, 5.90 μmol) instead of *p*-COOH-Bn-DO3A*i*Bu(^{t}Bu)$_3$. Purification by preparative RP-HPLC (system F, 27.7 min of retention time) provided DOTA-Bn-F as a white solid (0.6 mg, 0.875 μmol, 14.8%). HR-MS(ESI) calcd for $C_{33}H_{42}N_5O_{11}$ $[M-H]^-$: *m*/*z* 684.28808, found 684.28754. HPLC purity >99%, retention time 19.3 min (system A).

*Synthesis of FGK(Boc) and FGK(Mal) Conjugated with Chelators. FGK(Boc)-Trt(2-Cl)-Resin (**9**).* Compound **9** (0.900 mmol/g) was constructed by a conventional Fmoc solid-phase peptide synthesis on Trt(2-Cl)-Resin using *N,N′*-diisopropylcarbodiimide (DIC) and 1-hydroxybenzotriazole·monohydrate in dry DMF.[21]

*DO3AiBu-Bn-FGK (**10**).* A suspension of **9** (5.56 μmol/6.0 mg) was mixed with a mixture of *p*-COOH-Bn-DO3A*i*Bu(^{t}Bu)$_3$ (5.9 mg, 8.34 μmol, 1.5 equiv), 1-hydroxy-7-azabenzotriazole (HOAt, 1.5 mg, 5 equiv), and DIC (1.6 μL, 5 equiv) in DMF (0.2 mL) overnight at room temperature. After washing the resin with DMF (5.0 mL × 8) and dichloromethane (5.0 mL × 8), the peptide was cleaved from the resin by treatment with a mixture of TFA, water, and triisopropylsilane (95:2.5:2.5, v/v/v) for 2 h at room temperature. After the filtration, the filtrate was evaporated *in vacuo*. Diethyl ether (5.0 mL) was added to the residue to give the precipitate. The precipitate was purified by preparative RP-HPLC (system G, 24.8 min of retention time) to provide DO3A*i*Bu-Bn-FGK as a white solid (4.8 mg, 5.52 μmol, 99.3%). HR-MS(ESI) calcd for $C_{43}H_{63}N_8O_{11}$ $[M-H]^-$: *m*/*z* 867.46163, found: 867.46019.

*DOTA-Bn-FGK (**11**).* DOTA-Bn-FGK was prepared according to the same procedure as DO3A*i*Bu-Bn-FGK using *p*-COOH-Bn-DOTA-(^{t}Bu)$_4$ (20 mg, 26.2 μmol) instead of *p*-COOH-Bn-DO3A*i*Bu(^{t}Bu)$_3$. Purification by preparative RP-HPLC (system H, 30.2 min of retention time) provided DOTA-Bn-FGK as a white solid (12.0 mg, 13.8 μmol, 52.6%). HR-MS(ESI) calcd for $C_{41}H_{57}N_8O_{13}$ $[M-H]^-$: *m*/*z* 869.40451, found: 869.40483.

*DO3AiBu-Bn-FGK(Boc) (**12**).* To a solution of DO3A*i*Bu-Bn-FGK (2.0 mg, 2.30 μmol) in saturated aqueous sodium hydrogen carbonate (200 μL) was added a solution of $(Boc)_2O$ (1.0 mg, 2.0 equiv) in dioxane (200 μL) and stirred for 2 h at room temperature. After removing the solvent *in vacuo*, water was added to the residue and washed with chloroform (2 mL × 3). The aqueous phase was purified by preparative RP-HPLC (system G, 34.7 min of retention time) to provide DO3A*i*Bu-Bn-FGK(Boc) as a white solid (1.2 mg, 0.842 μmol, 53.8%). HR-MS(ESI) calcd for $C_{48}H_{71}N_8O_{13}$ $[M-H]^-$: *m*/*z* 967.51406, found 967.51052. HPLC purity 95.5%, retention time 23.9 min (system A).

*DOTA-Bn-FGK(Boc) (**13**).* DOTA-Bn-FGK(Boc) was prepared according to the same procedure as DO3A*i*Bu-Bn-FGK(Boc) using DOTA-Bn-FGK (0.5 mg, 0.574 μmol) instead of DO3A*i*Bu-Bn-FGK. Purification by preparative RP-HPLC (system I, 32.0 min of retention time) provided DOTA-Bn-FGK(Boc) as a white solid (0.4 mg, 0.412 μmol, 71.8%). HR-MS(ESI) calcd for $C_{46}H_{65}N_8O_{15}$ $[M-H]^-$: *m*/*z* 969.45694, found: 969.45796. HPLC purity >99%, retention time 19.3 min (system A).

*DO3AiBu-Bn-FGK(Mal) (**14**).* To a chilled (0 °C) solution of DO3A*i*Bu-Bn-FGK (1.8 mg, 2.07 μmol) in saturated aqueous sodium hydrogen carbonate (200 μL) was added *N*-methoxycarbonylmaleimide (1.6 mg, 5 equiv) and stirred for 2 h at the same temperature. The pH of the solution was adjusted to around 3 with 10% citric acid and purified by preparative RP-HPLC (system J, 30.7 min of retention time) to provide DO3A*i*Bu-Bn-FGK(Mal) as a white solid (0.8 mg, 0.843 μmol, 40.7%). HR-MS(ESI) calcd for $C_{47}H_{63}N_8O_{13}$ $[M-H]^-$: *m*/*z* 947.45146, found: 947.45417. HPLC purity 99.0%, retention time 23.1 min (system A).

*DOTA-Bn-FGK(Mal) (**15**).* DOTA-Bn-FGK(Mal) was prepared according to the same procedure as DO3A*i*Bu-Bn-FGK(Mal) using DOTA-Bn-FGK (2.4 mg, 2.76 μmol) instead of DO3A*i*Bu-Bn-FGK. Purification by preparative RP-HPLC (system K, 34.3 min of retention time) provided DOTA-Bn-FGK(Mal) as a white solid (0.7 mg, 0.736 μmol, 26.7%). HR-MS(ESI) calcd for $C_{45}H_{57}N_8O_{15}$ $[M-H]^-$: *m*/*z* 949.39434, found: 949.39464. HPLC purity >99%, retention time 22.0 min (system A).

Radiolabeling of Low-Molecular-Weight Compounds with ^{111}In. When the samples for log *D* measurements were prepared, [^{111}In]$InCl_3$ was used after concentration in a rotary evaporator. [^{111}In]$InCl_3$ (25 μL, 1.85 or 14.8 MBq) was dissolved in 1 M acetate buffer (pH 5.5, 25 μL) and allowed to stand for 5 min at room temperature to prepare [^{111}In]In-acetate. A solution of [^{111}In]In-acetate (50 μL) was added to a 100 μM solution of DO3A*i*Bu-Bn-F, DOTA-Bn-F, DO3A*i*Bu-Bn-FGK(Boc), DOTA-Bn-FGK(Boc), and DOTA-Bn-SCN-K in 0.1 M acetate buffer (pH 5.5, 50 μL) and kept to react for 5 min at 95 °C. After cooling to room temperature, a 50 mM DTPA solution was added to the mixture at a final concentration of 500 μM. The mixture was allowed to stand for 5 min and then purified using analytical RP-HPLC. All of the compounds provided two isomers, and each isomer was isolated with radiochemical purity greater than 97% (Figures S2 and S3). Retention time of analytical HPLC: 21.0 and 22.0 min (system A), 26.2 and 27.3 min (system D) for [^{111}In]In-DO3A*i*Bu-Bn-F, 18.2 and 19.0 min (system A), 20.9 and 21.4 min (system D) for [^{111}In]In-DOTA-Bn-F, 25.8 and 26.2 min (system A), 34.9 and 35.9 min (system D) for [^{111}In]In-DO3A*i*Bu-Bn-FGK(Boc), 24.0 and 24.4 min (system A), 31.7 and 32.3 min (system D) for [^{111}In]In-DOTA-Bn-FGK(Boc), 19.8 and 20.6 min (system A) for [^{111}In]In-DO3A*i*Bu-Bn-FG, and 10.5 and 10.7 min (system A), 18.5 and 19.1 min (system B) for [^{111}In]In-DOTA-Bn-SCN-K.

Log *D* Measurements. In this experiment, each isomer of [^{111}In]In-DO3A*i*Bu-Bn-F and [^{111}In]In-DOTA-Bn-F was not isolated, and mixtures of the isomers were used. A 5 μL (1.85 MBq) aliquot of [^{111}In]In-DO3A*i*Bu-Bn-F or [^{111}In]In-DOTA-Bn-F was mixed with equal amounts (3.0 mL) of 1-octanol and 25 mM phosphate buffer (pH 7.0 or 5.5). The mixture was vortexed for 1 min and allowed to stand for 1 min. After repeating the procedure five times, the mixture was centrifuged at 1500*g* for 10 min. Aliquots of 1.0 mL were taken from each phase and their radioactivity was measured with an auto-well γ counter. The partition coefficient was determined by calculating the ratio of the counts per minute in the 1-octanol phase to that in the buffer phase and expressed as common logarithm. The results represent the mean of three measurements for each compound.

***In Vitro* Metabolic Study of ^{111}In-Labeled LMW Substrates.** BBM vesicles were isolated from the renal cortex of male Wistar rats using the Mg/EDTA precipitation method as reported previously.[25] The enzyme-mediated cleavages of the FGK linkages in [^{111}In]In-DO3A*i*Bu-Bn-FGK(Boc) and [^{111}In]In-DOTA-Bn-FGK(Boc) were determined according to our previous procedures with slight modifications.[25] Briefly, a solution of BBM vesicles (10 μL, 1 mg/mL for [^{111}In]In-DO3A*i*Bu-Bn-FGK(Boc) and 10 mg/mL for [^{111}In]In-DOTA-Bn-FGK(Boc)) was incubated for 10 min at 37 °C before the addition of each ^{111}In-labeled derivative (10 μL). After 2 h of incubation at 37 °C, the radiolabeled species in the reaction mixture were analyzed by RP-TLC (Figure S3). An aliquot of the reaction mixture was applied to a 10 kDa cutoff ultrafiltration membrane, centrifuged at 10,000*g* for 20 min, and the filtrate was analyzed by RP-HPLC. Similar experiments were performed in the presence of 1 mM captopril (Fujifilm Wako Pure Chemical Corporation).

Preparation of Chelator-Conjugated Fab. DO3A*i*Bu-Bn-FGK-Fab and DOTA-Bn-FGK-Fab were synthesized by the maleimide-thiol chemistry as described previously with some modifications:[45] Briefly, a solution of Fab (100 μL, 4 mg/mL) in 0.16 M borate buffer (pH 8.0) containing 2 mM EDTA was preincubated for 10 min and reacted with 10 μL of 2-iminothiolane solution (1.92 mg/mL, Nacalai Tesque) in the same buffer for 30 min at 37 °C. After the reaction, excess 2-iminothiolane was removed by a centrifuged column procedure using Sephadex G-50 fine (GE Healthcare) equilibrated and eluted with 0.1 M phosphate buffer (pH 6.0) containing 2 mM EDTA to provide a solution of thiolated Fab. Aliquots of this mixture were sampled to estimate the number of thiol groups with 2,2′-dipyridyl disulfide (Tokyo Chemical Industry).[46] DO3A*i*Bu-Bn-FGK(Mal) or DOTA-Bn-FGK(Mal) (10 μL, 15 mg/mL in the same buffer as thiolated Fab) was added to the filtrate (90 μL) and then mixed gently for 1 h at 37 °C. Excess chelators were removed by the centrifuged column procedure using Sephadex G-50 fine equilibrated and eluted with 0.1 M phosphate buffer (pH 6.0) containing 2 mM EDTA, and aliquots of the filtrate

https://doi.org/10.1021/acs.jmedchem.3c00258
J. Med. Chem. 2023, 66, 8600−8613

were then sampled to estimate the number of thiol groups with DPS. After 5 μL of iodoacetamide (55.4 mg/mL, Fujifilm Wako Pure Chemical Corporation) in phosphate buffer (pH 6.0) was added, the reaction mixture was further incubated for 1 h to alkylate the unreacted thiol groups. DO3A*i*Bu-Bn-FGK-Fab and DOTA-Bn-FGK-Fab were subsequently purified by the centrifuged column procedure using a Sephadex G-50 fine equilibrated and eluted with 0.25 M acetate buffer (pH 5.5).

DOTA-Bn-SCN-Fab was synthesized by the same procedure described previously with some modifications:[29] Briefly, a solution of Fab (100 μL, 5 mg/mL) in 0.16 M borate buffer (pH 8.5) was reacted with 14 μL of *p*-SCN-Bn-DOTA solution (10 mg/mL) in the same buffer (pH adjusted to 8.5) at 4 °C overnight. DOTA-Bn-SCN-Fab was purified by the centrifuged column procedure using Sephadex G-50 fine equilibrated and eluted with 0.25 M acetate buffer (pH 5.5). The number of *p*-SCN-Bn-DOTA introduced per molecule was measured by the same procedure described previously.[30]

Preparation of ^{111}In-Labeled Fab. [^{111}In]$InCl_3$ was used after concentration in a rotary evaporator. An aliquot of [^{111}In]$InCl_3$ (15 μL, 8.9−13.3 MBq) was mixed with 1 M acetate buffer (pH 5.5, 5 μL) and incubated for 5 min at room temperature. A 10 μL solution of [^{111}In]In-acetate was added to each solution of DO3A*i*Bu-Bn-FGK-Fab (7.5 μL, 1.14 mg/mL), DOTA-Bn-FGK-Fab (7.5 μL, 1.82 mg/mL), and DOTA-Bn-SCN-Fab (7.5 μL, 3.39 mg/mL) in 0.25 M acetate buffer (pH 5.5) and kept to react for 1 h at 40 °C. After the reaction, a 50 mM DTPA solution was added to the mixture to achieve a final concentration of 500 μM. Each mixture was allowed to stand for 5 min and purified by a centrifuged column procedure using Sephadex G-50 fine (GE Healthcare) equilibrated and eluted with D-PBS(−) (Nacalai Tesque) to provide a solution of ^{111}In-labeled Fab.

***In Vitro* Stability of ^{111}In-Labeled Fab in Mouse Plasma.** A solution of ^{111}In-labeled Fab (18.5 kBq/0.5 μg/10 μL) was added to 90 μL of freshly prepared murine plasma, and the mixture was incubated at 37 °C. After incubation for 1, 3, 6, and 24 h, aliquots were withdrawn and analyzed by RP-TLC.

***In Vivo* Stability of ^{111}In-Labeled Fab in Mouse Plasma.** A solution of [^{111}In]In-DO3A*i*Bu-Bn-FGK-Fab, [^{111}In]In-DOTA-Bn-FGK-Fab, or [^{111}In]In-DOTA-Bn-SCN-Fab in D-PBS(−) (740 kBq/5 μg/100 μL) was injected via the tail vein into 6-week-old male ddY mice (24−26 g). The mice were anesthetized using isoflurane, and the blood samples at 3 h postinjection were collected by cardiac puncture. The blood samples were centrifuged at 1500*g* for 10 min. An aliquot of the plasma samples was analyzed by RP-TLC.

***In Vitro* Competitive Inhibition Assay.** [^{125}I]I-Fab was prepared by the chloramine T method.[34] A competitive inhibition assay was performed as described previously.[41] Briefly, [^{125}I]I-Fab, [^{111}In]In-DO3A*i*Bu-Bn-FGK-Fab, or [^{111}In]In-DOTA-Bn-SCN-Fab (20 kcpm) was incubated with 3 × 10^6 SY cells in the presence of different concentrations of unlabeled antibodies (0.5, 1, 2.5, 5, 10, 25, 50 nM) for 1 h on ice. The cells were centrifuged and washed twice with 1% BSA/PBS. The radioactivity bound to the cells was counted, and the IC_{50} values were determined by GraphPad Prism 8.4.3.

Biodistribution of ^{111}In-Labeled Fab in Normal Mice. A solution of [^{111}In]In-DO3A*i*Bu-Bn-FGK-Fab, [^{111}In]In-DOTA-Bn-FGK-Fab, or [^{111}In]In-DOTA-Bn-SCN-Fab in D-PBS(−) (11 kBq/5 μg/100 μL) was injected via the tail vein into 6-week-old male ddY mice (24−26 g). Groups of five mice were sacrificed at 10 min, 1, 3, 6, or 24 h postinjection. The organs of interest were removed and weighed, and the radioactivity was estimated using an auto-well gamma counter (Wizard 3, PerkinElmer Japan). Urine and fecal samples were collected for 6 and 24 h postinjection, and the radioactivities of these samples were also estimated.

Analysis of Urinary Radioactivity. A solution of [^{111}In]In-DO3A*i*Bu-Bn-FGK-Fab, [^{111}In]In-DOTA-Bn-FGK-Fab, or [^{111}In]In-DOTA-Bn-SCN-Fab in D-PBS(−) (296 kBq/5 μg/100 μL) was injected via the tail vein into 6-week-old male ddY mice (24−26 g) and urine samples were collected for 6 h. An aliquot of the urine samples was filtered by a 0.45 μm membrane filter and analyzed by SE-HPLC. Urine samples (100 μL) were also analyzed by RP-HPLC after filtration through a 10 kDa cutoff ultrafiltration membrane.

Analysis of Renal Radioactivity. A solution of [^{111}In]In-DO3A*i*Bu-Bn-FGK-Fab, [^{111}In]In-DOTA-Bn-FGK-Fab, or [^{111}In]In-DOTA-Bn-SCN-Fab in D-PBS(−) (296−333 kBq/5 μg/100 μL) was injected via the tail vein into 6-week-old male ddY mice (24−26 g). The mice were treated according to the procedure described by Uehara et al. at 10 min postinjection.[45]

Biodistribution of ^{111}In-Labeled Fab in Tumor-Bearing Mice. Five-week-old BALB/c nu/nu mice were xenografted subcutaneously into their right hind legs by injecting SY cells (2.5 × 10^6 cells) suspended in Matrigel (BD Biosciences). On achieving a tumor diameter of approximately 10 mm, these mice (21−24 g) were subjected to biodistribution and SPECT/CT imaging studies. A solution of ^{111}In-DO3A*i*Bu-Bn-FGK-Fab or ^{111}In-DOTA-Bn-SCN-Fab in D-PBS(−) (11 kBq/5 μg/100 μL) was injected via the tail vein into the tumor-bearing mice. Groups of six mice were sacrificed at 3 h postinjection. The organs of interest were removed and weighed, and the radioactivity was estimated using an auto-well gamma counter (Wizard 3).

SPECT/CT Imaging. A solution of [^{111}In]In-DO3A*i*Bu-Bn-FGK-Fab or [^{111}In]In-DOTA-Bn-SCN-Fab in D-PBS(−) (2 MBq/10 μg/100 μL) was injected via the tail vein into SY-tumor-bearing mice. After 150 min of injection of each ^{111}In-labeled Fab, SPECT and X-ray CT imaging were performed using a small animal SPECT/CT system (SPECT4/CT, Trifoil Imaging) equipped with five pinhole (1.0 mm) collimators. During SPECT and CT imaging, the mice were anesthetized with isoflurane (1.5%, 1 L/min). SPECT data acquisition was performed at 240 s per projection, with a stepwise rotation of 16 projections over 360°. SPECT images were reconstructed using three-dimensional-ordered subset expectation maximization (3D-OSEM) algorithms with four subsets and eight iterations.

Statistical Analysis. Data are presented as mean ± SD. Biodistribution studies in normal mice were analyzed using one-way analysis of variance (ANOVA) followed by Tukey's multiple-comparison test (GraphPad Prism 8.4.3). *In vitro* metabolic studies and biodistribution studies in tumor-bearing mice were analyzed using the Student's *t*-test (GraphPad Prism 8.4.3).

■ ASSOCIATED CONTENT

Supporting Information

The Supporting Information is available free of charge at https://pubs.acs.org/doi/10.1021/acs.jmedchem.3c00258.

Synthetic procedures of DO3A*i*Bu-Bn-FG, DOTA-Bn-SCN-K, and nonradioactive In-labeled compounds; log *D* values of [^{111}In]In-DO3A*i*Bu-Bn-F and [^{111}In]In-DOTA-Bn-F (Table S1); plasma stability of ^{111}In-labeled Fabs (Table S2); biodistribution results of [^{111}In]In-DO3A*i*Bu-Bn-FGK-Fab (Table S3), [^{111}In]In-DOTA-Bn-FGK-Fab (Table S4), and [^{111}In]In-DOTA-Bn-SCN-Fab (Table S5) in normal mice; biodistribution results of [^{111}In]In-DO3A*i*Bu-Bn-FGK-Fab and [^{111}In]In-DOTA-Bn-SCN-Fab in SY-tumor-bearing mice (Table S6); biodistribution results of [^{111}In]In-DO3A*i*Bu-Bn-F (Table S7) and [^{111}In]In-DOTA-Bn-F (Table S8) in normal mice; RP-HPLC chromatograms of **6** and the precursors used for radiolabeling reactions (Figure S1); RP-HPLC and SE-HPLC radiochromatograms of radiolabeled compounds (Figure S2); RP-TLC radiochromatograms of radiolabeled compounds (Figure S3); RP-HPLC and RP-TLC radiochromatograms after incubation of isomers A′, B′, C′, and D′ with BBM vesicles (Figure S4); RP-HPLC chromatograms for characterization of radiolabeled compounds (Figure S5); SE-HPLC chromatograms for characterization of ^{111}In-labeled Fabs (Figure S6); RP-TLC analyses of the plasma samples at 3 h postinjection of ^{111}In-labeled Fabs (Figure

https://doi.org/10.1021/acs.jmedchem.3c00258
J. Med. Chem. 2023, 66, 8600−8613

S7); and *in vitro* competitive inhibition assay of radiolabeled Fabs (Figure S8) (PDF)

Molecular formula strings (CSV)

AUTHOR INFORMATION

Corresponding Author

Hiroyuki Suzuki − *Laboratory of Molecular Imaging and Radiotherapy, Graduate School of Pharmaceutical Sciences, Chiba University, Chiba 260-8675, Japan;* orcid.org/0000-0002-9560-4274; Email: h.suzuki@chiba-u.jp

Authors

Mari Araki − *Laboratory of Molecular Imaging and Radiotherapy, Graduate School of Pharmaceutical Sciences, Chiba University, Chiba 260-8675, Japan*

Kouki Tatsugi − *Laboratory of Molecular Imaging and Radiotherapy, Graduate School of Pharmaceutical Sciences, Chiba University, Chiba 260-8675, Japan*

Kento Ichinohe − *Laboratory of Molecular Imaging and Radiotherapy, Graduate School of Pharmaceutical Sciences, Chiba University, Chiba 260-8675, Japan*

Tomoya Uehara − *Laboratory of Molecular Imaging and Radiotherapy, Graduate School of Pharmaceutical Sciences, Chiba University, Chiba 260-8675, Japan;* orcid.org/0000-0002-1140-9800

Yasushi Arano − *Laboratory of Molecular Imaging and Radiotherapy, Graduate School of Pharmaceutical Sciences, Chiba University, Chiba 260-8675, Japan;* orcid.org/0000-0001-6091-5382

Complete contact information is available at: https://pubs.acs.org/10.1021/acs.jmedchem.3c00258

Author Contributions

The manuscript was written through the contributions of all authors. All authors have given approval to the final version of the manuscript.

Notes

The authors declare no competing financial interest.

ACKNOWLEDGMENTS

The authors thank Hayahito Miyake for technical assistance. They also thank Editage (www.editage.com) for English language editing. This work was supported in part by a Grant-in-Aid for Scientific Research (B) (20H03619, to T.U.) from the Japan Society for the Promotion of Science (JSPS).

ABBREVIATIONS USED

ACE, angiotensin-converting enzyme; BBM, brush border membrane; COMU, {{[(1-cyano-2-ethoxy-2-oxoethylidene)-amino]oxy}-4-morpholinomethylene} dimethylammonium hexafluorophosphate; DIC, *N,N′*-diisopropylcarbodiimide; DIEA, *N,N*-diisopropylethylamine; DOTA, 1,4,7,10-tetraazacyclododecane-1,4,7,10-tetraacetic acid; HOAt, 1-hydroxy-7-azabenzotriazole; LMW Abs, low-molecular-weight antibody fragments and constructs; TEA, triethylamine; TFA, trifluoroacetic acid; RP-HPLC or RP-TLC, reversed-phase HPLC or TLC

REFERENCES

(1) Kelkar, S. S.; Reineke, T. M. Theranostics: combining imaging and therapy. *Bioconjugate Chem.* **2011**, *22*, 1879−1903.

(2) Witzig, T. E.; Flinn, I. W.; Gordon, L. I.; Emmanouilides, C.; Czuczman, M. S.; Saleh, M. N.; Cripe, L.; Wiseman, G.; Olejnik, T.; Multani, P. S.; White, C. A. Treatment with ibritumomab tiuxetan radioimmunotherapy in patients with rituximab-refractory follicular non-Hodgkin's lymphoma. *J. Clin. Oncol.* **2002**, *20*, 3262−3269.

(3) Werner, R. A.; Bluemel, C.; Allen-Auerbach, M. S.; Higuchi, T.; Herrmann, K. ^{68}Gallium-and ^{90}Yttrium-/^{177}Lutetium:"theranostic twins" for diagnosis and treatment of NETs. *Ann. Nucl. Med.* **2015**, *29*, 1−7.

(4) Kulkarni, H. R.; Singh, A.; Langbein, T.; Schuchardt, C.; Mueller, D.; Zhang, J.; Lehmann, C.; Baum, R. P. Theranostics of prostate cancer: from molecular imaging to precision molecular radiotherapy targeting the prostate specific membrane antigen. *Br. J. Radiol.* **2018**, *91*, No. 20180308.

(5) Parakh, S.; Lee, S. T.; Gan, H. K.; Scott, A. M. Radiolabeled Antibodies for Cancer Imaging and Therapy. *Cancers* **2022**, *14*, 1454.

(6) Milenic, D.; Yokota, T.; Filpula, D.; Finkelman, M.; Dodd, S.; Wood, J.; Whitlow, M.; Snoy, P.; Schlom, J. Construction, binding properties, metabolism, and tumor targeting of a single-chain Fv derived from the pancarcinoma monoclonal antibody CC49. *Cancer Res.* **1991**, *51*, 6363−6371.

(7) Yokota, T.; Milenic, D. E.; Whitlow, M.; Schlom, J. Rapid tumor penetration of a single-chain Fv and comparison with other immunoglobulin forms. *Cancer Res.* **1992**, *52*, 3402−3408.

(8) Orlova, A.; Magnusson, M.; Eriksson, T. L.; Nilsson, M.; Larsson, B.; Höidén-Guthenberg, I.; Widström, C.; Carlsson, J.; Tolmachev, V.; Ståhl, S.; Nilsson, F. Y. Tumor imaging using a picomolar affinity HER2 binding affibody molecule. *Cancer Res.* **2006**, *66*, 4339−4348.

(9) Ståhl, S.; Gräslund, T.; Karlström, A. E.; Frejd, F. Y.; Nygren, P.-Å.; Löfblom, J. Affibody molecules in biotechnological and medical applications. *Trends Biotechnol.* **2017**, *35*, 691−712.

(10) Behr, T. M.; Goldenberg, D. M.; Becker, W. Reducing the renal uptake of radiolabeled antibody fragments and peptides for diagnosis and therapy: present status, future prospects and limitations. *Eur. J. Nucl. Med. Mol. Imaging* **1998**, *25*, 201−212.

(11) Akizawa, H.; Uehara, T.; Arano, Y. Renal uptake and metabolism of radiopharmaceuticals derived from peptides and proteins. *Adv. Drug Delivery Rev.* **2008**, *60*, 1319−1328.

(12) Behr, T. M.; Sharkey, R. M.; Sgouros, G.; Blumenthal, R. D.; Dunn, R. M.; Kolbert, K.; Griffiths, G. L.; Siegel, J. A.; Becker, W. S.; Goldenberg, D. M. Overcoming the nephrotoxicity of radiometal-labeled immunoconjugates: improved cancer therapy administered to a nude mouse model in relation to the internal radiation dosimetry. *Cancer* **1997**, *80*, 2591−2610.

(13) Arano, Y. Renal brush border strategy: A developing procedure to reduce renal radioactivity levels of radiolabeled polypeptides. *Nucl. Med. Biol.* **2021**, *92*, 149−155.

(14) Arano, Y.; Fujioka, Y.; Akizawa, H.; Ono, M.; Uehara, T.; Wakisaka, K.; Nakayama, M.; Sakahara, H.; Konishi, J.; Saji, H. Chemical design of radiolabeled antibody fragments for low renal radioactivity levels. *Cancer Res.* **1999**, *59*, 128−134.

(15) Uehara, T.; Koike, M.; Nakata, H.; Hanaoka, H.; Iida, Y.; Hashimoto, K.; Akizawa, H.; Endo, K.; Arano, Y. Design, synthesis, and evaluation of [^{188}Re]organorhenium-labeled antibody fragments with renal enzyme-cleavable linkage for low renal radioactivity levels. *Bioconjugate Chem.* **2007**, *18*, 190−198.

(16) Uehara, T.; Yokoyama, M.; Suzuki, H.; Hanaoka, H.; Arano, Y. Gallium-67/68-labeled antibody fragments for immuno-SPECT/PET show low renal radioactivity without loss of tumor uptake. *Clin. Cancer Res.* **2018**, *24*, 3309−3316.

(17) Suzuki, H.; Kise, S.; Watanabe, R.; Sugawa, T.; Furukawa, T.; Nakano, N.; Fujii, H.; Uehara, T. Cupper-64-labeled antibody fragments for immuno-PET/radiotherapy with low renal radioactivity levels and amplified tumor-kidney ratios. *ACS Omega* **2021**, *6*, 21556−21562.

(18) Suzuki, C.; Uehara, T.; Kanazawa, N.; Wada, S.; Suzuki, H.; Arano, Y. Preferential cleavage of a tripeptide linkage by enzymes on renal brush border membrane to reduce renal radioactivity levels of radiolabeled antibody fragments. *J. Med. Chem.* **2018**, *61*, 5257−5268.

(19) Uehara, T.; Kanazawa, N.; Suzuki, C.; Mizuno, Y.; Suzuki, H.; Hanaoka, H.; Arano, Y. Renal Handling of ^{99m}Tc-Labeled Antibody Fab Fragments with a Linkage Cleavable by Enzymes on Brush Border Membrane. *Bioconjugate Chem.* **2020**, *31*, 2618−2627.
(20) Price, E. W.; Orvig, C. Matching chelators to radiometals for radiopharmaceuticals. *Chem. Soc. Rev.* **2014**, *43*, 260−290.
(21) Suzuki, H.; Ichinohe, K.; Araki, M.; Muramatsu, S.; Uehara, T.; Arano, Y. Synthesis and evaluation of a *para*-carboxylated benzyl-DOTA for labeling peptides and polypeptides. *Nucl. Med. Biol.* **2022**, *114-115*, 18−28.
(22) Mohsin, H.; Fitzsimmons, J.; Shelton, T.; Hoffman, T. J.; Cutler, C. S.; Lewis, M. R.; Athey, P. S.; Gulyas, G.; Kiefer, G. E.; Frank, R. K.; et al. Preparation and biological evaluation of ^{111}In-, ^{177}Lu-and ^{90}Y-labeled DOTA analogues conjugated to B72. 3. *Nucl. Med. Biol.* **2007**, *34*, 493−502.
(23) D'huyvetter, M.; Aerts, A.; Xavier, C.; Vaneycken, I.; Devoogdt, N.; Gijs, M.; Impens, N.; Baatout, S.; Ponsard, B.; Muyldermans, S.; et al. Development of ^{177}Lu-nanobodies for radioimmunotherapy of HER2-positive breast cancer: evaluation of different bifunctional chelators. *Contrast Media Mol. Imaging* **2012**, *7*, 254−264.
(24) Maguire, W. F.; McDevitt, M. R.; Smith-Jones, P. M.; Scheinberg, D. A. Efficient 1-step radiolabeling of monoclonal antibodies to high specific activity with ^{225}Ac for α-particle radioimmunotherapy of cancer. *J. Nucl. Med.* **2014**, *55*, 1492−1498.
(25) Fujioka, Y.; Satake, S.; Uehara, T.; Mukai, T.; Akizawa, H.; Ogawa, K.; Saji, H.; Endo, K.; Arano, Y. In vitro system to estimate renal brush border enzyme-mediated cleavage of Peptide linkages for designing radiolabeled antibody fragments of low renal radioactivity levels. *Bioconjugate Chem.* **2005**, *16*, 1610−1616.
(26) Suzuki, H.; Kanai, A.; Uehara, T.; Gomez, F. L. G.; Hanaoka, H.; Arano, Y. Facile synthesis and evaluation of *C*-functionalized benzyl-1-oxa-4,7,10-triazacyclododecane-*N*,*N*′,*N*″-triacetic acid as chelating agent for ^{111}In-labeled polypeptides. *Bioorg. Med. Chem.* **2012**, *20*, 978−984.
(27) Schlesinger, J.; Koezle, I.; Bergmann, R.; Tamburini, S.; Bolzati, C.; Tisato, F.; Noll, B.; Klussmann, S.; Vonhoff, S.; Wuest, F.; et al. An ^{86}Y-labeled mirror-image oligonucleotide: influence of Y-DOTA isomers on the biodistribution in rats. *Bioconjugate Chem.* **2008**, *19*, 928−939.
(28) Mani, T.; Tircsó, G.; Zhao, P.; Sherry, A. D.; Woods, M. Effect of the regiochemistry of butyl amide substituents on the solution-state structures of lanthanide(III) DOTA-tetraamide complexes. *Inorg. Chem.* **2009**, *48*, 10338−10345.
(29) Cooper, M. S.; Sabbah, E.; Mather, S. J. Conjugation of chelating agents to proteins and radiolabeling with trivalent metallic isotopes. *Nat. Protoc.* **2006**, *1*, 314.
(30) Dadachova, E.; Chappell, L.; Brechbiel, M. Spectrophotometric method for determination of bifunctional macrocyclic ligands in macrocyclic ligand−protein conjugates. *Nucl. Med. Biol.* **1999**, *26*, 977−982.
(31) Ehlers, M. R. W.; Riordan, J. F. Angiotensin-converting enzyme: new concepts concerning its biological role. *Biochemistry* **1989**, *28*, 5311−5318.
(32) Ronca-Testoni, S. Direct spectrophotometric assay for angiotensin-converting enzyme in serum. *Clin. Chem.* **1983**, *29*, 1093−1096.
(33) Rice, G. I.; Jones, A. L.; Grant, P. J.; Carter, A. M.; Turner, A. J.; Hooper, N. M. Circulating activities of angiotensin-converting enzyme, its homolog, angiotensin-converting enzyme 2, and neprilysin in a family study. *Hypertension* **2006**, *48*, 914−920.
(34) Arano, Y.; Wakisaka, K.; Ohmono, Y.; Uezono, T.; Akizawa, H.; Nakayama, M.; Sakahara, H.; Tanaka, C.; Konishi, J.; Yokoyama, A. Assessment of radiochemical design of antibodies using an ester bond as the metabolizable linkage: evaluation of maleimidoethyl 3-(tri-*n*-butylstannyl) hippurate as a radioiodination reagent of antibodies for diagnostic and therapeutic applications. *Bioconjugate Chem.* **1996**, *7*, 628−637.
(35) Arano, Y.; Inoue, T.; Mukai, T.; Wakisaka, K.; Sakahara, H.; Konishi, J.; Yokoyama, A. Discriminated release of a hippurate-like radiometal chelate in nontarget tissues for target-selective radioactivity localization using pH-dependent dissociation of reduced antibody. *J. Nucl. Med.* **1994**, *35*, 326−333.
(36) Brandt, F.; Ullrich, M.; Wodtke, J.; Kopka, K.; Bachmann, M.; Löser, R.; Pietzsch, J.; Pietzsch, H.-J. R.; Wodtke, R. Enzymological Characterization of ^{64}Cu-Labeled Neprilysin Substrates and Their Application for Modulating the Renal Clearance of Targeted Radiopharmaceuticals. *J. Med. Chem.* **2023**, *66*, 516−537.
(37) Fujioka, Y.; Arano, Y.; Ono, M.; Uehara, T.; Ogawa, K.; Namba, S.; Saga, T.; Nakamoto, Y.; Mukai, T.; Konishi, J.; Saji, H. Renal metabolism of 3′-iodohippuryl N^{ε}-maleoyl-L-lysine (HML)-conjugated Fab fragments. *Bioconjugate Chem.* **2001**, *12*, 178−185.
(38) Del Prete, M.; Buteau, F.-A.; Beauregard, J.-M. Personalized ^{177}Lu-octreotate peptide receptor radionuclide therapy of neuroendocrine tumours: a simulation study. *Eur. J. Nucl. Med. Mol. Imaging* **2017**, *44*, 1490−1500.
(39) Zhang, M.; Jacobson, O.; Kiesewetter, D. O.; Ma, Y.; Wang, Z.; Lang, L.; Tang, L.; Kang, F.; Deng, H.; Yang, W.; et al. Improving the Theranostic Potential of Exendin 4 by Reducing the Renal Radioactivity through Brush Border Membrane Enzyme-Mediated Degradation. *Bioconjugate Chem.* **2019**, *30*, 1745−1753.
(40) Bendre, S.; Zhang, Z.; Kuo, H.-T.; Rousseau, J.; Zhang, C.; Merkens, H.; Roxin, Á.; Bénard, F.; Lin, K.-S. Evaluation of Met-Val-Lys as a renal brush border enzyme-cleavable linker to reduce kidney uptake of ^{68}Ga-labeled DOTA-conjugated peptides and peptidomimetics. *Molecules* **2020**, *25*, 3854.
(41) Sogawa, C.; Tsuji, A. B.; Sudo, H.; Sugyo, A.; Yoshida, C.; Odaka, K.; Uehara, T.; Arano, Y.; Koizumi, M.; Saga, T. C-kit-targeted imaging of gastrointestinal stromal tumor using radiolabeled anti-c-kit monoclonal antibody in a mouse tumor model. *Nucl. Med. Biol.* **2010**, *37*, 179−187.
(42) Yoshida, C.; Tsuji, A. B.; Sudo, H.; Sugyo, A.; Kikuchi, T.; Koizumi, M.; Arano, Y.; Saga, T. Therapeutic efficacy of c-kit-targeted radioimmunotherapy using 90Y-labeled anti-c-kit antibodies in a mouse model of small cell lung cancer. *PLoS One* **2013**, *8*, No. e59248.
(43) Boldrini, L.; Ursino, S.; Gisfredi, S.; Faviana, P.; Donati, V.; Camacci, T.; Lucchi, M.; Mussi, A.; Basolo, F.; Pingitore, R. Expression and mutational status of c-kit in small-cell lung cancer: prognostic relevance. *Clin. Cancer Res.* **2004**, *10*, 4101−4108.
(44) Hirota, S.; Isozaki, K.; Moriyama, Y.; Hashimoto, K.; Nishida, T.; Ishiguro, S.; Kawano, K.; Hanada, M.; Kurata, A.; Takeda, M.; et al. Gain-of-function mutations of c-kit in human gastrointestinal stromal tumors. *Science* **1998**, *279*, 577−580.
(45) Uehara, T.; Rokugawa, T.; Kinoshita, M.; Nemoto, S.; Fransisco Lazaro, G. G.; Hanaoka, H.; Arano, Y. $^{67/68}$Ga-labeling agent that liberates $^{67/68}$Ga-NOTA-methionine by lysosomal proteolysis of parental low molecular weight polypeptides to reduce renal radioactivity levels. *Bioconjugate Chem.* **2014**, *25*, 2038−2045.
(46) Grassetti, D. R.; Murray, J., Jr. Determination of sulfhydryl groups with 2,2′- or 4,4′-dithiodipyridine. *Arch. Biochem. Biophys.* **1967**, *119*, 41−49.

https://doi.org/10.1021/acs.jmedchem.3c00258
J. Med. Chem. 2023, 66, 8600−8613